J. Fluid Mech. (1997), *vol.* 334, *pp.* 211–249

Moving contact lines in liquid/liquid/solid systems

By YULII D. SHIKHMURZAEV†

Institute of Mechanics, Moscow University, 119899 Moscow, Russia

(Received 13 December 1994 and in revised form 17 June 1996)

A general mathematical model which describes the motion of an interface between immiscible viscous fluids along a smooth homogeneous solid surface is examined in the case of small capillary and Reynolds numbers. The model stems from a conclusion that the Young equation, $\sigma_1 \cos\theta = \sigma_2 - \sigma_3$, which expresses the balance of tangential projections of the forces acting on the three-phase contact line in terms of the surface tensions σ_i and the contact angle θ, together with the well-established experimental fact that the dynamic contact angle deviates from the static one, imply that the surface tensions of contacting interfaces in the immediate vicinity of the contact line deviate from their equilibrium values when the contact line is moving. The same conclusion also follows from the experimentally observed kinematics of the flow, which indicates that liquid particles belonging to interfaces traverse the three-phase interaction zone (i.e. the 'contact line') in a finite time and become elements of another interface – hence their surface properties have to relax to new equilibrium values giving rise to the surface tension gradients in the neighbourhood of the moving contact line. The kinematic picture of the flow also suggests that the contact-line motion is only a particular case of a more general phenomenon – the process of interface formation or disappearance – and the corresponding mathematical model should be derived from first principles for this general process and then applied to wetting as well as to other relevant flows. In the present paper, the simplest theory which uses this approach is formulated and applied to the moving contact-line problem. The model describes the true kinematics of the flow so that it allows for the 'splitting' of the free surface at the contact line, the appearance of the surface tension gradients near the contact line and their influence upon the contact angle and the flow field. An analytical expression for the dependence of the dynamic contact angle on the contact-line speed and parameters characterizing properties of contacting media is derived and examined. The role of a 'thin' microscopic residual film formed by adsorbed molecules of the receding fluid is considered. The flow field in the vicinity of the contact line is analysed. The results are compared with experimental data obtained for different fluid/liquid/solid systems.

1. Introduction

In the present paper we consider the moving contact-line problem for a general liquid/liquid/solid system, i.e. in the situation where two immiscible viscous liquids are in contact with a solid surface and one of the liquids displaces the other so that

† Present address: Department of Applied Mathematical Studies, University of Leeds, Leeds LS2 9JT, UK.

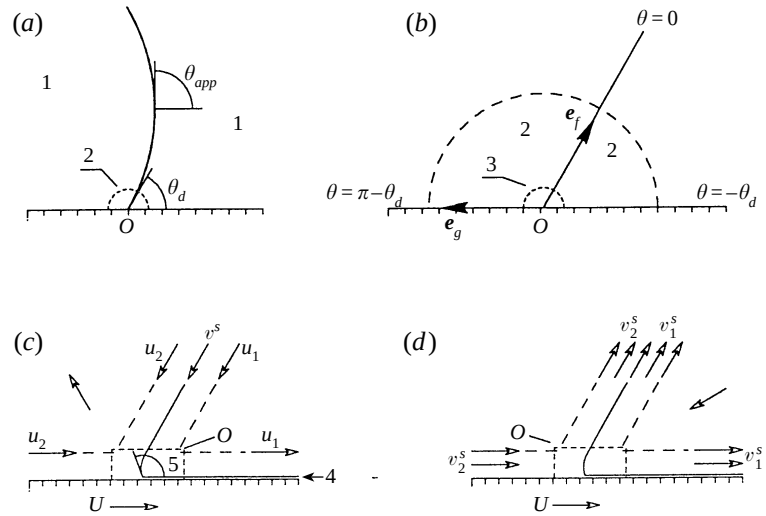

FIGURE 1. Definition sketches of the flow in the neighbourhood of the contact line with interfaces shown as layers of finite thickness. Views (*c*) and (*d*) correspond to the situation where the advancing fluid 'rolls over' and the receding fluid 'unrolls from' the solid surface, respectively. Asymptotic regions 1, 2, 3 are associated with characteristic length scales 1, ϵ and ϵCa, respectively; 4 is the microscopic residual film; 5 is the microscopic (or actual) contact angle θ_{act}; θ_d and θ_{app} are the macroscopic and apparent contact angle, respectively; O is the three-phase interaction zone (the 'contact line'). The plane polar coordinate system (r, θ) is fixed with respect to the contact line. Subscripts 1 and 2 refer to the advancing and receding fluid, respectively.

the contact line (where the liquid–liquid interface intersects the solid boundary) is constrained to move across the solid surface. The problem is important both from a purely theoretical and a practical point of view and attracts the attention of many investigators.

Experiments show the following. (i) One of the liquids (which one depends on the viscosity ratio and the dynamic-contact-angle value) undergoes so-called *rolling* motion (figure 1) so that a liquid element initially adjacent to the free surface becomes adjacent to the liquid–solid interface (or vice versa) in a finite time while in the other liquid the flow has a 'jet-like' structure with the bulk velocity directed from (or towards) the contact line (the liquid–liquid interface 'splits' at the contact line, see Dussan V. & Davis 1974; Dussan V. 1979 for details). (ii) The dynamic contact angle θ_d measured through the advancing liquid increases as the contact-line speed grows (Elliott & Riddiford 1967; Blake & Haynes 1969; Hansen & Toong 1971; Gutoff & Kendrick 1982; Fermigier & Jenffer 1991).

A theoretical analysis of the liquid–liquid displacement on the basis of the classical approach, with the no-slip boundary conditions for velocities of both liquids on the solid surface, the capillarity equation and continuity of tangential velocity and stress on the free surface, encounters a fundamental difficulty. Consideration of the flow field in the neighbourhood of the moving contact line shows that in the general case the problem has no solution, while if the capillarity equation is dropped and the free-surface shape is prescribed, then a solution appears but it contains a non-integrable singularity in the shear stress at the contact line resulting in a divergent integral for the drag force experienced by the solid wall. This problem is known in the literature as the 'moving contact-line problem'.

Mathematical models proposed for resolving the moving contact-line problem may be conventionally classified from the point of view of the characteristic length scale they are dealing with. The works devoted to the *microhydrodynamics* of wetting consider the flow in the neighbourhood of the contact line on the length scale comparable with the thickness of interfacial layers, and therefore must explicitly take into account the diffuse nature of interfaces and, in particular, the forces of a non-hydrodynamic origin which act on such length scales (see de Gennes 1985; Starov 1992 for reviews). However, the forces of a non-hydrodynamic origin (such as, for example, the van der Waals forces) are unable to eliminate the shear-stress singularity in the general formulation of the moving contact-line problem, i.e. if the Navier–Stokes or Stokes equations are used without simplifications to describe the flow in the bulk; this is clear, for example, from the analysis carried in Dussan V. & Davis (1974). At the same time, if the problem is considered in the framework of the lubrication approximation, which in itself simplifies the singularity and reduces it to the singularity of the bulk pressure, then the singularity can be suppressed by a proper choice of an additional, also singular, pressure caused by non-hydrodynamic forces. It should be pointed out however that, strictly speaking, the lubrication approximation (which is simply a mathematical tool for obtaining an approximation of the exact solution) should not become a remedy for singularities caused by the physical nature of the problem: it may be applied only if the non-simplified problem has a regular solution. Microhydrodynamic models usually deal either with the case of perfectly wetting fluids, where the solid surface is assumed to be covered by a precursor film hyperbolically decaying to zero (and hence there is no actual contact line and no stress singularity) or with the case of a partially wetting fluid, where, as was pointed out above, the singularity cannot be removed with the introduction of intermolecular forces only, and the fundamental difficulty is the same as in conventional hydrodynamics. On microhydrodynamic length scales (see, for example, Hocking 1995) the long-range intermolecular forces strongly influence both the flow field and the *apparent* contact angle – an auxiliary concept used for interpreting experimental observations.

Macrohydrodynamics of wetting deals with flows on length scales large compared not only with the interfacial layer thickness but also with characteristic dimensions of surface roughness elements or chemical inhomogeneities (Hocking 1976; Huh & Mason 1977*a*; Jansons 1985, 1986, 1988; Joanny & Robbins 1990). The main goal of macrohydrodynamics is to reduce the problem of the wetting of an actual rough solid surface to consideration of an 'effective' contact-line motion across some 'effective' smooth boundary. Details of the actual flow over the surface roughness elements are either not considered or assumed to be known. This problem has much in common with the corresponding problem of the mechanics of multiphase systems (Jansons 1985).

The present paper as well as most others (see Dussan V. 1979; Shikhmurzaev 1993*a* and §9 of the present paper for reviews) consider the *hydrodynamics* of the liquid–liquid displacement, i.e. the flow on length scales large compared with the interfacial layer thickness over the actual (not 'effective') surface of a solid. Very often in this case it is convenient to illustrate the properties of a model by considering the flow over a perfectly smooth chemically homogeneous solid surface. This case is also of practical importance since, from the point of view of fluid mechanics, some surfaces, such as for example freshly cleaved mica and crystal faces, may be regarded as smooth, and they are widely used in experiments and applications. Another example of smooth surfaces are those produced by the vacuum deposition technique.

In the present paper, a model proposed for the description of the moving contact line in gas/liquid/solid systems (Shikhmurzaev 1991*a*, 1993*a*, 1994, 1996†) is generalized and applied to the liquid–liquid displacement process. The scope is to present a model which includes the previously developed model as a particular case, eliminates the shear-stress singularity at the contact line, describes the qualitative features of phenomena (i), (ii), and is in reasonable quantitative agreement with experimental data. The theory is formulated on the basis of the following physical ideas.

(*a*) According to the true kinematics of the flow (see (i)), liquid elements which form the interfaces traverse the three-phase interaction region (the 'contact line') in a finite time, and therefore their surface properties (such as, for example, the surface tension) have to relax to new equilibrium values giving rise to surface tension gradients in the immediate vicinity of the contact line.

(*b*) The deviation of the dynamic contact angle away from the static one (see (ii)) together with the tangential momentum balance law expressed by the classical Young equation also imply that the surface tensions of contacting interfaces in the vicinity of the moving contact line are not in equilibrium.

(*c*) The surface tension relaxation time is a macroscopic quantity (see, for example, Kochurova, Shvechenkov & Rusanov 1974 and references therein) so that relaxation occurs not within the three-phase interaction zone (which is described as the 'contact line' on the hydrodynamic length scale) but along the interfaces, as also follows from the arguments given above.

(*d*) The surface tension gradients along the interfaces in the vicinity of the moving contact line are caused by the flow and will have the reverse influence upon the flow which caused them (the flow-induced Marangoni effect).

These ideas indicate that the moving-contact-line problem is only a particular case of a more general phenomenon – the process of interface formation or disapperance – which should be described from first principles. The simplest self-consistent model of this process was derived in Shikhmurzaev (1993*a*,*b*). In the present paper, we will illustrate how the model can be applied to the moving-contact-line problem for a general fluid/liquid/solid system. In §2 a general formulation of the problem applicable to flows at finite capillary and Reynolds numbers is presented. Section 3 is devoted to the simplifications which become possible in the case of small relaxation lengths, capillary and Reynolds numbers. In §4 analytical expressions for the dependence of the drag force and the dynamic contact angle on the contact-line speed and other parameters of the problem are derived, and §5 is devoted to their analysis. In §6 we consider different definitions of the dynamic contact angle and, in particular, discuss correlations between the present theory and an approach which uses the concept of 'apparent contact angle' for interpretation of experiments. Preliminary quantitative comparison of the theory with experimental data is carried out in §7. Section 8 deals with the flow field in the vicinity of a moving contact line. In §9, existing hydrodynamic theories are briefly reviewed and compared with the present model. It is shown in particular that the 'seeds' of the model developed in this paper are present in many of the earlier theories. In §10 we briefly discuss limitations of the theory and possible ways to eliminate them.

† Note a misprint in the sign of the surface pressure gradient in equation (6). The subsequent formulae are correct.

2. General formulation of the problem

We will consider a flow in the neighbourhood of a moving contact line formed at the intersection of an interface between two immiscible viscous liquids and an ideally smooth chemically homogeneous solid surface. The characteristic dimensions of the flow are assumed to be large compared with the thickness of the interfacial layers so that these layers may be described as geometrical surfaces of zero thickness. In the subsequent sections we will use the subscripts 1 and 2 to mark parameters of the advancing and receding liquid respectively, but in the present section the problem will be formulated in a symmetrical form so that the problem statement can be applied for an arbitrary direction of the contact-line motion. The superscript s refers to the *surface* parameters which describe properties of interfaces such as, for example, the surface tension. The flow is considered in the coordinate frame fixed with respect to the contact line.

If ρ_i, $\boldsymbol{u}_i$, p_i and μ_i are the density, velocity, pressure and viscosity of the ith liquid and $\boldsymbol{I}$ is the metric tensor, then in the absence of gravity effects the bulk flow is described by

$$\left.\begin{aligned} \nabla\cdot\boldsymbol{u}_i = 0, \qquad \rho_i\left(\frac{\partial\boldsymbol{u}_i}{\partial t} + \boldsymbol{u}_i\cdot\nabla\boldsymbol{u}_i\right) &= \nabla\cdot\boldsymbol{P}_i, \\ \boldsymbol{P}_i = -p_i\boldsymbol{I} + \mu\left(\nabla\boldsymbol{u} + (\nabla\boldsymbol{u})^T\right), \qquad i &= 1,2. \end{aligned}\right\} \tag{2.1}$$

The effects of gravity could be readily taken into account: then (2.1) are still valid so long as p_1 and p_2 are interpreted as the excess pressure over hydrostatic.

General boundary conditions for both liquids ($i = 1, 2$) on the solid surface which were formulated in Shikhmurzaev (1993*a*) include the following.

(i) The generalization of the Navier boundary condition

$$\boldsymbol{n}\cdot\boldsymbol{P}_i\cdot(\boldsymbol{I} - \boldsymbol{nn}) - \tfrac{1}{2}\nabla p_i^s = \beta_i(\boldsymbol{u}_i - \boldsymbol{U})\cdot(\boldsymbol{I} - \boldsymbol{nn}), \tag{2.2}$$

where $\boldsymbol{n}$ is an outward normal to the solid surface (so that $\boldsymbol{n}\cdot\boldsymbol{P}_i\cdot(\boldsymbol{I} - \boldsymbol{nn})$ is the shear stress exerted on the liquid–solid interface by the ith liquid), p_i^s is the surface pressure (i.e. a two-dimensional pressure in a thin layer of the liquid adjacent to the solid surface which is caused, as is the surface tension on the free surface, by the asymmetric action of intermolecular forces from bulk phases), β_i is the coefficient of sliding friction (Lamb 1932, p. 586; Bedeaux, Albano & Mazur 1976), and $\boldsymbol{U}$ is the velocity of the solid.

(ii) The surface equation of state

$$p_i^s = \gamma_i(\rho_i^s - \rho_{i0}^s), \tag{2.3}$$

which is given here in the simplest form describing only the dependence of the surface pressure on the surface density ρ_i^s (γ_i is a phenomenological coefficient, and ρ_{i0}^s is the surface density corresponding to zero surface pressure).

(iii) The surface mass balance equation

$$\frac{\partial\rho_i^s}{\partial t} + \nabla\cdot(\rho_i^s\boldsymbol{v}_i^s) = -\frac{\rho_i^s - \rho_{is}^s}{\tau_i}, \tag{2.4}$$

where ρ_{is}^s is the equilibrium surface density determined by the nature of contacting media; $\boldsymbol{v}_i^s$ is the surface velocity, and τ_i is the relaxation time.

(iv) Equations of the Darcy type which relate components of the surface velocity $\boldsymbol{v}_i^s$ to components of the bulk velocities evaluated on the opposite sides of the liquid–solid

interface and the surface pressure gradient

$$\left.\begin{aligned} \boldsymbol{v}_i^s \cdot (\boldsymbol{I} - \boldsymbol{nn}) = \tfrac{1}{2}(\boldsymbol{u}_i + \boldsymbol{U}) \cdot (\boldsymbol{I} - \boldsymbol{nn}) - \alpha_i \nabla p_i^s, \\ (\boldsymbol{v}_i^s - \boldsymbol{U}) \cdot \boldsymbol{n} = (\boldsymbol{u}_i - \boldsymbol{v}_i^s) \cdot \boldsymbol{n} = 0, \end{aligned}\right\} \tag{2.5}$$

where α_i is a phenomenological coefficient, which characterizes in an integral form the influence of the surface pressure gradient on the velocity distribution across the interfacial layer.

The right-hand side of (2.4) describes the interface formation process. In the present model, the surface density is actually not a measure of inertial properties of interfaces (see (2.5)), and it is used simply as a parameter which characterizes the current state of the interface (see (2.3)) and in principle can be excluded from the set of boundary conditions by means of (2.3). Some possible ways for the experimental determination of the surface equation of state are discussed in Shikhmurzaev (1996).

Obviously, mass exchange between the interface and the bulk may be neglected in the boundary conditions for the bulk velocity (see (2.5)). Experiments show (see, for example, Posner & Alexander 1949; Kochurova *et al.* 1974) that, both for solutions and pure liquids, a characteristic time of relaxation of interface properties is rather large ($\sim 10^{-3}$ s), and hence the surface tension relaxation 'tail' should be surprisingly long. The experimental values of τ_i slightly exceed those estimated from an order-of-magnitude analysis in Shikhmurzaev (1993*a*). Some possible ways of generalizing the theory are discussed also in Shikhmurzaev (1994).

Our modelling of the free surface will take into account that the interfacial layer between immiscible liquids is composed by two sublayers (figure 1*c*,*d*) each having its own surface properties so that, for example, the total surface pressure, defined as a quantity equal in value and opposite in sign to the surface tension, is given by $p^s = p_1^s + p_2^s$, where p_i^s and ρ_i^s are related by the equations of state (2.3).

General boundary conditions on the interface between immiscible viscous liquids derived in the same way as (2.2)–(2.5) (see Shikhmurzaev 1993*b*) include the following.

(i) The momentum balance equation for a free surface element

$$\nabla \cdot \boldsymbol{P}^s + \boldsymbol{n} \cdot (\boldsymbol{P}_1 - \boldsymbol{P}_2) = 0, \tag{2.6}$$

where a unit normal vector $\boldsymbol{n}$ points from liquid 2 to liquid 1, and

$$\boldsymbol{P}^s = -(p_1^s + p_2^s)(\boldsymbol{I} - \boldsymbol{nn}).$$

(ii) The surface mass balance equations

$$\frac{\partial \rho_i^s}{\partial t} + \nabla \cdot (\rho_i^s \boldsymbol{v}_i^s) = -\frac{\rho_i^s - \rho_{if}^s}{\tau_i}, \tag{2.7}$$

where ρ_{if}^s $(i = 1, 2)$ are the equilibrium surface densities of components in the sublayers.

(iii) Equations, analogous to (2.5), which relate components of the surface velocities with the bulk velocities evaluated on the opposite sides of the interface

$$\boldsymbol{v}_i^s \cdot (\boldsymbol{I} - \boldsymbol{nn}) = \tfrac{1}{2}(\boldsymbol{u}_i + \boldsymbol{v}^s) \cdot (\boldsymbol{I} - \boldsymbol{nn}) - \alpha_i \nabla p_i^s, \qquad (\boldsymbol{v}_i^s - \boldsymbol{v}^s) \cdot \boldsymbol{n} = (\boldsymbol{u}_i - \boldsymbol{v}^s) \cdot \boldsymbol{n} = 0 \tag{2.8}$$

(here $\boldsymbol{v}^s$ is the velocity on the surface separating the sublayers).

(iv) Equations which relate the difference between bulk velocities on the opposite sides of the interface with the surface pressure gradients and shear stresses experienced by the interface (a generalization of (2.2))

$$(-1)^{i+1} \boldsymbol{n} \cdot \boldsymbol{P}_i \cdot (\boldsymbol{I} - \boldsymbol{nn}) - \tfrac{1}{2} \nabla p_i^s = \beta_i (\boldsymbol{u}_i - \boldsymbol{v}^s) \cdot (\boldsymbol{I} - \boldsymbol{nn}). \tag{2.9}$$

(v) The angular momentum equation for a free surface element

$$\nabla p_1^s = \nabla p_2^s. \tag{2.10}$$

The normal projection of (2.6) gives the well-known equation of capillarity; the tangential projection relates the difference between the shear stresses acting on the opposite sides of the interface with the surface tension gradient (the Marangoni effect). It is evident that in the 'outer' region associated with the limit $\epsilon_i \equiv U\tau_i/L \to 0$ $(i = 1, 2)$ with $\mu_i/(\beta_i L) = o(1)$ (L is the characteristic length scale of the flow domain), the relationships (2.2)–(2.10) for the main terms of asymptotic expansions in ϵ_i become the classical boundary conditions usually formulated for the Navier–Stokes equations, i.e. the no-slip condition on solid boundaries and the equation of capillarity, zero normal velocities and continuity for tangential velocities and stresses on free surfaces. An analysis of the orders of magnitude for the coefficients involved in (2.6)–(2.10) can be found in Shikhmurzaev (1993*a*, *b*). Relationships (2.2), (2.4), (2.5) and the corresponding formulae for the liquid–gas interface (Shikhmurzaev 1993*a*, 1994, 1996) can be obtained from (2.6)–(2.10) as the limiting cases.

For stationary processes the time derivatives in (2.4), (2.7) (as well as in (2.1)) disappear, while if we were to consider the interface formation processes, which take place, for example, when two media are instantaneously brought in contact, the time derivatives would be necessary and initial distributions of the surface densities (or the surface tensions) should be prescribed.

The distributions of the surface parameters must be linked by some boundary conditions at the contact line. We will attribute no *line* parameters to the contact line (e.g. a line density, line tension, etc) though in certain cases such a generalization may be of interest (see Marmur 1983 for a discussion). The boundary conditions at the contact line include (*a*) the mass balance equations for the fluxes of both components into and out of the contact-line region; (*b*) the balance condition for the tangential forces acting on the contact line (the Young equation for the dynamic condition).

The mass balance condition at the contact line should take into account one peculiarity of the liquid–liquid displacement process: the moving contact line in liquid/liquid/solid systems may be followed by a microscopic residual film (figure 1*c*,*d*) formed by adsorbed molecules of the displaced liquid (Teletzke, Davis & Scriven 1988). We will consider the case of a microscopic film thin compared with the interfacial layer thickness ($\rho_{res}^s \ll \rho_{1s}^s, \rho_{2s}^s$, where ρ_{res}^s is the surface density of the residual film) so that its influence on boundary conditions (2.2)–(2.5) may be neglected. At the same time, if $\rho_{res}^s \sim \rho_{if}^s - \rho_{is}^s$, $(i = 1, 2)$, then the microscopic residual film (if present) must be taken into account in the mass balance condition at the contact line. The sensitiveness of the macroscopic characteristics of the moving-contact-line problem in the case of gas/liquid/solid systems to the surface mass fluxes due to microscopic residual films is shown in Shikhmurzaev (1996). A possible way of generalizing the theory for the case of a 'thick microscopic' residual film is discussed in §10.

Thus, the mass balance conditions at an arbitrary point $\boldsymbol{r}_0$ of the contact line in a reference frame where the contact-line speed is zero may be written down for both components in a unified form as follows:

$$(\rho_i^s \boldsymbol{v}_i^s)|_{\boldsymbol{r}\to\boldsymbol{r}_0, \boldsymbol{r}\in\Sigma} \cdot \boldsymbol{e}_f + (-1)^i (\rho_i^s \boldsymbol{v}_i^s)|_{\boldsymbol{r}\to\boldsymbol{r}_0, \boldsymbol{r}\in S} \cdot \boldsymbol{e}_g + k_i \rho_{res}^s \boldsymbol{U} \cdot \boldsymbol{e}_g = 0 \quad (i = 1, 2). \tag{2.11}$$

Here ρ_{res}^s is the surface density of the ('thin') microscopic residual film formed by molecules of the receding liquid; $k_1 = 1$, $k_2 = 0$ if $\boldsymbol{U} \cdot \boldsymbol{e}_g > 0$ and $k_1 = 0$, $k_2 = -1$ if $\boldsymbol{U} \cdot \boldsymbol{e}_g < 0$ (this can be formally expressed in terms of the Heaviside function $\vartheta(x)$ as $k_i = 1 - i + \vartheta(\boldsymbol{U} \cdot \boldsymbol{e}_g)$ for $i = 1, 2$); Σ and S denote the liquid–liquid and liquid–solid

interface, respectively; the notation $\boldsymbol{r} \to \boldsymbol{r}_0$, $\boldsymbol{r} \in \Sigma$(or S) is used to denote the limit of a function as $\boldsymbol{r}$ tends to $\boldsymbol{r}_0$ along Σ(or S); $\boldsymbol{e}_f$ and $\boldsymbol{e}_g$ are the unit vectors normal to the contact line and directed along the free surface and the interface between liquid 2 and the solid, respectively. The dynamic contact angle θ_d measured through liquid 1 is defined by

$$\cos\theta_d = -\boldsymbol{e}_f \cdot \boldsymbol{e}_g.$$

It should be pointed out that (2.11) allows for 'splitting' of the liquid–liquid interface at the contact line and therefore makes possible the rolling motion of at least one of the liquids over the solid surface (see (i) in §1).

The momentum balance condition for an element of the contact line projected on the direction normal to the contact line and tangential to the solid surface takes the usual form of the Young equation

$$(p_1^s + p_2^s)|_{\boldsymbol{r}\to\boldsymbol{r}_0,\,\boldsymbol{r}\in\Sigma}\,\boldsymbol{e}_f \cdot \boldsymbol{e}_g = (p_1^s|_{\boldsymbol{r}\to\boldsymbol{r}_0,\,\boldsymbol{r}\in S} + p_{2S}^s) - (p_2^s|_{\boldsymbol{r}\to\boldsymbol{r}_0,\,\boldsymbol{r}\in S} + p_{1S}^s). \tag{2.12}$$

Here for the sake of symmetry we have decomposed the component of the reaction force acting on the contact-line element tangential to the solid surface from the solid p_S^s into two parts

$$p_S^s = p_{1S}^s - p_{2S}^s, \tag{2.13}$$

which represent the forces experienced by liquid 1 and liquid 2 in the three-phase interaction zone. A simple order-of-magnitude analysis shows that for non-singular surface densities the convective momentum fluxes may be neglected and so the terms of the form $\rho^s v^{s2}$ do not appear in (2.12). Naturally, if the contact line is moving, the surface pressures p_i^s $(i = 1, 2)$ change due to the surface density variations according to (2.2)–(2.5). The Young theory implies that the component normal to the solid boundary of the force acting along the free surface is always balanced by a reaction force from the solid.

The system (2.1)–(2.13) must be completed by some boundary conditions far from the contact line and initial conditions if a non-stationary process is considered. It is evident that (2.2) guarantees the absence of the shear stress singularity at the contact line, and (2.11) allows the rolling motion of the liquids. It should be pointed out that the first term on the left-hand side of (2.2) may be regarded as a 'payment' for the simplification of the flow domain shape adopted. The present model tolerates a reformulation which preserves its macroscopic properties and makes the shear stress in (2.2) unimportant (see Shikhmurzaev 1991*a*,*b*; Shikhmurzaev 1994, p. 55 and §9 of the present paper). In the next section we consider the conditions for determining which liquid, advancing or receding, undergoes the rolling motion, and in §8 analyse the flow field in the vicinity of the contact line.

Boundary conditions (2.2)–(2.13) include those proposed for describing the motion of an interface between a viscous liquid and a viscous or inviscid gas (Shikhmurzaev 1993*a*, 1994, 1996) as a particular case. In that case, the interface consists only of material particles of the liquid so that all the 'surface parameters of the gas' vanish.

3. Small relaxation lengths, capillary and Reynolds numbers

We will consider the case of a steady flow when the velocity components parallel to the contact line are zero. It is assumed that the Reynolds and capillary numbers

for the two liquids are small,

$$Re_i \equiv \frac{\rho_i U L}{\mu_i} \ll 1, \; Ca_i \equiv \frac{\mu_i U}{\sigma} \ll 1 \quad (i = 1, 2), \tag{3.1}$$

$$\sigma \equiv -(p_1^s(\rho_{1f}^s) + p_2^s(\rho_{2f}^s)), \tag{3.2}$$

and the relaxation lengths $l_1 \equiv U\tau_1$ and $l_2 \equiv U\tau_2$ are much smaller than a macroscopic length scale L which characterizes the geometry of the flow domain (the capillary gap, the dimension of a droplet, etc). In this case, the moving contact-line problem may be considered as local (see Cox 1986 for details), and the left-hand side of the second equation (2.1) may be neglected everywhere ($Re_i \ll 1$). Since the set of equations (2.1)–(2.13) is singularly perturbed as $\epsilon_i \equiv l_i/L \to 0$ and $Ca_i \to 0$ ($i = 1, 2$), we may study the problem using the technique of matched asymptotic expansions. As $\epsilon_1 \to 0$ and $Ca_1 \to 0$ with $k_\tau \equiv \tau_2/\tau_1$ and $k_\mu \equiv \mu_2/\mu_1$ fixed, we may distinguish the following three asymptotic regions: the 'outer' region associated with the length scale L; the 'intermediate' region with the characteristic length scale $\epsilon_1 L$; the 'inner' (or 'viscous') region with the length scale $\epsilon_1 Ca_1 L$.

Solutions in these regions must be asymptotically matched. The union of the 'inner' and 'intermediate' regions will be called the 'slip' region since in this region the deviation from the classical no-slip boundary conditions takes place. Below only the terms of $O(1)$ as $Re,\ Ca,\ \epsilon \to 0$ are considered, and we will assume that $Ca \ln(\epsilon^{-1}) = o(1)$ as $Ca \to 0,\ \epsilon \to 0$ so that the solutions in the 'outer' and 'slip' asymptotic regions can be matched directly (see Cox 1986 and §6 for more details). Since k_τ and k_μ are assumed to be of $O(1)$, we will drop the subscript i where this will not cause misunderstandings).

3.1. *The 'outer' region*

Relationships (2.2)–(2.10) for the main terms of asymptotic expansions in ϵ_1 as $\epsilon_1 \to 0$ with r/L fixed (r is the value of a position vector) and $\mu_i/(\beta_i L) = o(1),\ i = 1, 2$, reduce to the classical boundary conditions for the bulk parameters and give that the surface quantities have their equilibrium values. Considering the normal projection of (2.6) in the limit $Ca_1 \to 0$ with $k_\mu = O(1)$, one obtains that the free surface is locally plane for sufficiently small r/L (so long as we consider terms of $O(1)$ as $\epsilon, Ca \to 0$). The asymptotic form of the velocity field as $r/L \to 0$ can be obtained by defining stream functions $\psi_{1(0)}$ and $\psi_{2(0)}$ such that $u_{ir(0)}$ and $u_{i\theta(0)}$, the radial and transverse components of $\boldsymbol{u}_i$ ($i = 1, 2$) in a plane polar coordinate system (r, θ) with the origin coincident with the projection of the contact line on the flow plane and the axis $\theta = 0$ directed along the free surface (figure 1), are

$$u_{ir(0)} = \frac{1}{r}\frac{\partial \psi_{i(0)}}{\partial \theta}, \quad u_{i\theta(0)} = -\frac{\partial \psi_{i(0)}}{\partial r} \quad (i = 1, 2). \tag{3.3}$$

The subscript 0 in parentheses hereafter refers to the functions representing the inner limit of the outer solution.

Substituting (3.3) in (2.1) with the inertial terms neglected and eliminating the pressure, one obtains biharmonic equations for the stream functions,

$$\nabla^4 \psi_{i(0)} = 0 \quad (i = 1, 2). \tag{3.4}$$

In the 'outer' region, equations (2.2) and (2.5) reduce to the usual no-slip boundary

conditions on the solid wall, which give

$$\psi_{1(0)} = 0, \quad \frac{\partial \psi_{1(0)}}{\partial \theta} = rU \quad \text{on } \theta = -\theta_d; \tag{3.5}$$

$$\psi_{2(0)} = 0, \quad \frac{\partial \psi_{2(0)}}{\partial \theta} = -rU \quad \text{on } \theta = \pi - \theta_d. \tag{3.6}$$

Here U is the speed of the solid in the chosen coordinate frame and θ_d is the dynamic contact angle measured through the advancing liquid; the value of θ_d is *a priori* unknown. In the 'outer' region conditions (2.8) and the tangential projection of (2.6) take the form

$$\psi_{1(0)} = \psi_{2(0)} = 0, \quad \frac{\partial \psi_{1(0)}}{\partial \theta} = \frac{\partial \psi_{2(0)}}{\partial \theta}, \quad \mu_1 \frac{\partial^2 \psi_{1(0)}}{\partial \theta^2} = \mu_2 \frac{\partial^2 \psi_{2(0)}}{\partial \theta^2} \text{ on } \theta = 0. \tag{3.7}$$

The solution of (3.4) which satisfies (3.5)–(3.7) is given by

$$\psi_{i(0)} = rUg_i(\theta), \quad (i = 1, 2), \tag{3.8}$$

$$g_1 = C_1(\theta - \theta_1)\sin\theta + C_2\theta\sin(\theta - \theta_1),$$

$$g_2 = C_3(\theta - \theta_2)\sin\theta + C_4\theta\sin(\theta - \theta_2),$$

where constants C_i $(i = 1, \ldots, 4)$ are determined as follows:

$$C_1 = \frac{\cos\theta_1 K(\theta_2) - k_\mu\,[\pi(\sin\theta_1 + \theta_1\cos\theta_1) + \cos\theta_1 K(\theta_1)]}{k_\mu(\theta_2 - \sin\theta_2\cos\theta_2)K(\theta_1) - (\theta_1 - \sin\theta_1\cos\theta_1)K(\theta_2)},$$

$$C_2 = \frac{1}{\theta_1}(1 - C_1\sin\theta_1),$$

$$C_3 = \frac{\theta_2}{K(\theta_2)}\left(\frac{\pi\sin\theta_1}{\theta_1\theta_2} + C_1\frac{K(\theta_1)}{\theta_1}\right),$$

$$C_4 = -\frac{1}{\theta_2}(1 + C_3\sin\theta_2),$$

$$\theta_1 = -\theta_d, \quad \theta_2 = \pi - \theta_d, \quad k_\mu = \frac{\mu_2}{\mu_1}, \quad K(\theta) = \theta^2 - \sin^2\theta.$$

Obviously, the inner limit of the outer solution (3.8) is common for different models of the contact-line motion (see, for example, Cox 1986), and we present it here in a symmetric dimensional form giving no preference to parameters of one of the liquids. This solution implies that no other boundaries or/and sources of motion are located close to the contact line. A detailed analysis of (3.8) is given in Huh & Scriven (1971). Below, we will use the notation $u_{r(0)}(\theta_d, k_\mu)$ for the radial component of the free-surface velocity associated with the inner limit of the outer solution.

Resolving the equation $u_{r(0)}(\theta_d, k_\mu) = 0$ with respect to k_μ and making use of (3.8), one can introduce a function

$$k_\mu^*(\theta_d) = -\frac{({\theta_2}^2 - \sin^2\theta_2)(\theta_1\cos\theta_1 - \sin\theta_1)}{({\theta_1}^2 - \sin^2\theta_1)(\theta_2\cos\theta_2 - \sin\theta_2)}, \tag{3.9}$$

which determines the boundary at which the character of the flow changes (Huh & Scriven 1971): if $k_\mu < k_\mu^*(\theta_d)$, the advancing liquid rolls over the solid ($u_{r(0)} < 0$, see §1), while $k_\mu > k_\mu^*(\theta_d)$ corresponds to the situation where the receding liquid unrolls from the solid boundary, $u_{r(0)} > 0$.

It should be emphasized that equations (3.4) and the classical boundary conditions

(3.5)–(3.7) simply provide an accumulation of the results of numerous experiments with Newtonian liquids under different conditions, and hence (3.8), (3.9) reflect general features of the mutual displacement of Newtonian fluids irrespectively of the particular model proposed for the contact-line motion.†

3.2. *The 'intermediate' region*

Now let us consider the 'slip' region. We will make the variables dimensionless using the following scaling quantities: l_1, U, $\mu_1 U/l_1$ (the characteristic bulk pressure), σ, ρ^s_{i0} (the characteristic surface density for the ith liquid). Making use of the normal projection of (2.6), we immediately obtain that the free surface in the 'intermediate' region is planar so long as we deal with the terms of $O(1)$ as $\epsilon, Ca \to 0$.

For a stationary process equations (2.1), boundary conditions (2.2), (2.9), the tangential projection of (2.6), (2.10), (2.4), (2.7), (2.5), (2.8), rewritten using (2.3), take the form (here the terms of $O(Ca)$ are held in order to demonstrate the structure of the equations and make clear the subsequent analysis)

$$\nabla \cdot \boldsymbol{u}_1 = 0, \qquad \nabla^2 \boldsymbol{u}_1 - \nabla p_1 = 0 \quad (r > 0,\ -\theta_d < \theta < 0), \tag{3.10}$$

$$\nabla \cdot \boldsymbol{u}_2 = 0, \quad k_\mu \nabla^2 \boldsymbol{u}_2 - \nabla p_2 = 0 \quad (r > 0,\ 0 < \theta < \pi - \theta_d), \tag{3.11}$$

$$(-1)^{i-1} \frac{2Ca_i}{\lambda_i(1+4A_i)} \frac{1}{r} \frac{\partial u_{ir}}{\partial \theta} - \frac{\mathrm{d}\rho^s_i}{\mathrm{d}r} = 4k_\tau{}^{1-i} V_i^2 (v^s_i - (-1)^{i-1}) \quad \text{on } \theta = \theta_i, \tag{3.12}$$

$$(-1)^{i} \frac{2Ca_i}{\lambda_i(1+4A_i)} \frac{1}{r} \frac{\partial u_{ir}}{\partial \theta} - \frac{\mathrm{d}\rho^s_i}{\mathrm{d}r} = 4k_\tau{}^{1-i} V_i^2 (v^s_i - v^s) \ \text{ on } \theta = 0,\ i = 1,2; \tag{3.13}$$

$$\sum_{i=1}^{2} \left(\lambda_i \frac{\mathrm{d}\rho^s_i}{\mathrm{d}r} + (-1)^{i-1} \frac{Ca_i}{r} \frac{\partial u_{ir}}{\partial \theta} \right) = 0, \quad \lambda_1 \frac{\mathrm{d}\rho^s_1}{\mathrm{d}r} = \lambda_2 \frac{\mathrm{d}\rho^s_2}{\mathrm{d}r} \qquad \text{on } \theta = 0, \tag{3.14}$$

$$\frac{\mathrm{d}}{\mathrm{d}r}(\rho^s_1 v^s_1) = -(\rho^s_1 - \rho^s_{1j}) \quad (j = f \text{ on } \theta = 0;\ j = s \text{ on } \theta = \theta_1), \tag{3.15}$$

$$k_\tau \frac{\mathrm{d}}{\mathrm{d}r}(\rho^s_2 v^s_2) = -(\rho^s_2 - \rho^s_{2j}) \quad (j = f \text{ on } \theta = 0,\ j = s \text{ on } \theta = \theta_2), \tag{3.16}$$

$$u_{ir} = 2v^s_i - (-1)^{i-1} + \frac{2A_i k_\tau{}^{i-1}}{(1+4A_i)V_i^2} \frac{\mathrm{d}\rho^s_i}{\mathrm{d}r} \quad \text{on } \theta = \theta_i,\ i = 1,2, \tag{3.17}$$

$$u_{ir} = 2v^s_i - v^s + \frac{2A_i k_\tau{}^{i-1}}{(1+4A_i)V_i^2} \frac{\mathrm{d}\rho^s_i}{\mathrm{d}r} \quad \text{on } \theta = 0,\ i = 1,2, \tag{3.18}$$

$$u_{i\theta} = 0 \quad \text{on } \theta = 0, \theta_i; \quad i = 1,2, \tag{3.19}$$

† Striking experimental results recently reported by Savelski *et al.* (1995) do not seem to be sufficient evidence to invalidate the results of all previous experimental studies accumulated in (3.8), (3.9), as well as previous experiments on wetting itself, for the following reasons at least: (i) information about how the continuous variation of the parameters could link the data with the (opposite) results of early experiments is absent, and one has to guess about the changes in the experimental conditions which give rise to the surprising behaviour of the flow; (ii) the values of the capillary and Reynolds numbers corresponding to each experimental point are not given, and the only argument for comparing the results with (3.8), (3.9) – the model 'should give at least a qualitatively accurate physical picture' (p. 125) – seems poorly convincing; (iii) interpretation of unsteady experiments requires a detailed analysis of inertial effects.

where the same notation is used for dimensionless variables, and

$$\lambda_i = \frac{\gamma_i \rho^s_{i0}}{\sigma},\ A_i = \alpha_i \beta_i,\ V_i = \left(\frac{\beta_i}{\rho^s_{i0}(1 + 4\alpha_i \beta_i)} \right)^{1/2} U \qquad (i = 1, 2).$$

The conditions (2.11), (2.12) at the moving contact line may be rewritten as

$$(\rho^s_i v^s_i)_{|r\to 0,\,\theta=0} + (\rho^s_i v^s_i)_{|r\to 0,\,\theta=\theta_i} + (i-1)\rho^s_{res} = 0 \quad (i = 1, 2), \tag{3.20}$$

$$(p^s_1 + p^s_2)_{|r\to 0,\,\theta=0} \cos\theta_d = p^s_{2|r\to 0,\,\theta=\theta_2} - p^s_{1|r\to 0,\,\theta=\theta_1} + p^s_S \quad (i = 1, 2), \tag{3.21}$$

where p^s_i are defined by the dimensionless equations (2.3), namely

$$p^s_i = \lambda_i(\rho^s_i - 1) \quad (i = 1, 2). \tag{3.22}$$

Matching conditions for the zeroth-order terms take the form

$$u_{ir} \to u_{ir(0)},\ u_{i\theta} \to u_{i\theta(0)} \qquad \text{as } r \to \infty\ (i = 1, 2), \tag{3.23}$$

$$v^s_i \to u_{r(0)},\ \rho^s_i \to \rho^s_{if} \qquad \text{on } \theta = 0 \text{ as } r \to \infty\ (i = 1, 2), \tag{3.24}$$

$$v^s_i \to (-1)^{i-1},\ \rho^s_i \to \rho^s_{is} \qquad \text{on } \theta = \theta_i \text{ as } r \to \infty\ (i = 1, 2). \tag{3.25}$$

In equilibrium, the total surface pressure at the liquid–liquid interface is given by (see (3.2), (3.22))

$$p^s_1(\rho^s_{1f}) + p^s_2(\rho^s_{2f}) \equiv \lambda_1(\rho^s_{1f} - 1) + \lambda_2(\rho^s_{2f} - 1) = -1, \tag{3.26}$$

and the Young equation (3.21) rewritten for statics relates p^s_S with the static contact angle θ_s and the equilibrium surface densities ρ^s_{is} $(i = 1, 2)$:

$$\cos\theta_s = \lambda_1(\rho^s_{1s} - 1) - \lambda_2(\rho^s_{2s} - 1) - p^s_S. \tag{3.27}$$

As $Ca_1 \to 0$, $k_\mu = O(1)$, the system (3.10)–(3.25) is singularly perturbed, and the application of the technique of matched asymptotic expansions in Ca 'splits' the 'slip' region into the 'intermediate' and 'inner' regions associated with the limits $Ca_1 \to 0$ with r fixed and $Ca_1 \to 0$ with $\tilde{r} \equiv r/Ca_1$ fixed, respectively. In the 'intermediate' region, the terms proportional to Ca in (3.12)–(3.14) disappear; then (3.14) can be integrated and, using (3.24), (3.26), we obtain

$$\rho^s_i \equiv \rho^s_{if} \qquad \text{for } i = 1, 2 \text{ on } \theta = 0 \tag{3.28}$$

so that

$$\lambda_1(\rho^s_1 - 1) + \lambda_2(\rho^s_2 - 1) \equiv -1 \qquad \text{on } \theta = 0. \tag{3.29}$$

Using (3.28), we obtain from (3.13), (3.15), (3.16), (3.24) that

$$v^s_i \equiv u_{r(0)} \qquad \text{for } i = 1, 2 \text{ on } \theta = 0. \tag{3.30}$$

The distribution of the surface parameters along the liquid–solid interface in the 'intermediate' region can be found from (3.15), (3.16) for $j = s$, $\theta = \theta_1, \theta_2$ and (3.12), rewritten for the parameters in the 'intermediate' region, as

$$\frac{\mathrm{d}\rho^s_i}{\mathrm{d}r} = 4{k_\tau}^{1-i} {V_i}^2((-1)^{i-1} - v^s_i) \qquad \text{on } \theta = \theta_i\ (i = 1, 2), \tag{3.31}$$

completed by matching conditions (3.25) and some boundary conditions for the inner limits of the solution, which appear as the result of considering the 'inner' solution and matching the solutions in the 'intermediate' and 'inner' regions. It is important to emphasize that (3.15), (3.16) and (3.31) are independent of the solution in the

bulk. The distribution of the bulk velocities along the interfaces can be found then from (3.17)–(3.19) so that they become the boundary conditions for the bulk flow equations. In the case of finite capillary numbers, the 'slip' region could not be split into the above-described asymptotic subregions, the free surface would be no longer locally planar, the inner limit of the outer solution would become strongly dependent on the overall flow, and the distribution of the surface parameters in the 'slip' region would become interrelated with the bulk flow.

3.3. *The 'inner' region*

We will mark the parameters in the 'inner' region with a tilde ($\sim$) and use for parameters in the 'intermediate' region the same notation as before. Using the inner variable

$$\tilde{r} = \frac{r}{Ca_1}$$

in (3.10)–(3.22), we readily obtain from (3.12), (3.13), (3.15), (3.16) that

$$\tilde{\rho}_i^s, \tilde{v}_i^s \equiv \text{const} \qquad (\theta = 0, \theta_i;\ i = 1, 2), \tag{3.32}$$

i.e. so long as terms of $O(1)$ as $Ca_1 \to 0$ are considered, $\tilde{\rho}_i^s$ (and hence $\tilde{p}_i^s$, see (3.22)) and $\tilde{v}_i^s$ are independent of $\tilde{r}$. Taking this into account and having in mind the matching conditions of the terms of $O(1)$ of the asymptotic expansions in Ca of the solutions in the 'inner' and 'intermediate' regions,

$$\lim_{\tilde{r}\to\infty} \tilde{\phi} = \lim_{r\to 0} \phi, \tag{3.33}$$

we conclude that conditions (3.20), (3.21) are valid for the terms of $O(1)$ of the solution in the 'intermediate' region, and so we obtain the missing boundary conditions for the inner limits of the solution determined by (3.15), (3.16) for $j = s$, $\theta = \theta_1, \theta_2$, (3.28), (3.30), (3.31).

Thus, the set of equations (3.15), (3.16) for $j = s$, $\theta = \theta_1, \theta_2$, (3.28), (3.30), (3.31) and boundary conditions (3.20), (3.21), (3.25) is closed, and it allows one to find the dependence of θ_d and, as will be shown below, the force acting between the liquids and the solid in the neighbourhood of the moving contact line, on the parameters of the problem by considering the solution in the *'intermediate'* region. Equation (3.27) relates the parameters of the problem with the static and dynamic contact-angle values.

4. Macroscopic characteristics

4.1. *The drag force*

The momentum balance equation for the liquid–solid interface is analogous to the first equation (2.6) derived for the liquid–liquid interface (Shikhmurzaev 1993*b*, 1994). The force exerted on the liquid–solid interface by the solid is equal to

$$\frac{\mathrm{d}p_i^s}{\mathrm{d}r} + (-1)^i \frac{Ca_i}{r} \frac{\partial u_{ir}}{\partial \theta} \qquad \text{on } \theta = \theta_i,\ i = 1, 2. \tag{4.1}$$

Here the force density is made dimensionless using $\sigma/(U\tau_1)$ as a scale.

In the 'intermediate' region, the second term in (4.1) is of $O(Ca)$, and so there for the main terms of asymptotic expansions in Ca we have

$$f_i(r) = \frac{\mathrm{d}p_i^s}{\mathrm{d}r} \qquad \text{on } \theta = \theta_i,\ i = 1, 2, \tag{4.2}$$

while in the 'inner' region both terms are of the same order, and the main terms of the force density are given by

$$\tilde{f}_i(\tilde{r}) = \frac{\mathrm{d}\tilde{\tilde{p}}_i^s}{\mathrm{d}\tilde{r}} - (-k_\mu)^{i-1}\frac{1}{\tilde{r}}\frac{\partial \tilde{u}_{ir}}{\partial \theta} \quad \text{on } \theta = \theta_i,\ i = 1, 2. \tag{4.3}$$

Here a double tilde marks the second term of the asymptotic expansion of p_i^s in Ca_1 as Ca_1 tends to zero in the 'inner' region. As was shown in §3, the first term, $\tilde{p}_i^s$, is independent of $\tilde{r}$.

Recall that (4.1)–(4.3) give expressions for the force density in the plane polar coordinate system. Let us determine the main approximation for the projection of the total drag force on the direction of the solid wall velocity in a Cartesian coordinate system. In this case, the total drag force F calculated using a uniformly valid solution is given by

$$\begin{aligned} F &= \sum_{i=1}^{2}(-1)^{i-1}\int_0^\infty [f_i(r) + \tilde{f}_i(r/Ca_1) - f_i(0)]\,\mathrm{d}r + O(Ca) \\ &= \sum_{i=1}^{2}(-1)^{i-1}\left(\int_0^\infty f_i(r)\,\mathrm{d}r + Ca_1\int_0^\infty [\tilde{f}_i(\tilde{r}) - f_i(0)]\,\mathrm{d}\tilde{r}\right) + O(Ca) \\ &= \sum_{i=1}^{2}(-1)^{i-1}[p_i^s(\rho_{is}^s) - p_i^s(\rho_i^s(0))] + O(Ca) \quad \text{as } Ca \to 0. \end{aligned} \tag{4.4}$$

It is not difficult to show by considering the solution in the 'inner' region that both terms on the right-hand side of (4.3) are finite and the integrals in (4.4) are convergent.

From a physical point of view, the relationship (4.4) is obvious. Indeed, though the force density in the 'inner' region is finite, and the contribution of the shear stress is of the same order as that of the surface pressure gradient, the dimensions of this region are small (of $O(Ca)$) compared with those of the 'intermediate' region, and, therefore, the contribution of the 'inner' region to the total force may be neglected so long as we consider the leading terms of the asymptotic expansions in Ca. In the 'intermediate' region, the force density is also finite, but there the contribution to the total force due to the shear stress is of $O(Ca)$ and therefore may be neglected compared with the contribution due to the surface tension gradients, which is of $O(1)$ as $Ca \to 0$. Thus, the main contribution to the force between the liquid and the solid in the neighbourhood of the moving contact line is due to the surface tension gradient in the 'intermediate' region and not to the shear stress.

Combining (4.4), (3.21), (3.22), (3.27) and (3.29), we finally obtain

$$F = \cos\theta_s - \cos\theta_d. \tag{4.5}$$

Thus, we have derived a well-known empirical correlation between the total drag force acting on the liquid in the vicinity of the contact line and the dynamic contact angle. This derivation makes clear the conditions of applicability of (4.5).

4.2. *The dynamic contact angle*

The set of equations and boundary conditions (3.15), (3.16) for $j = s$, $\theta = \theta_1, \theta_2$, (3.28), (3.30), (3.31), (3.20), (3.21), (3.25) is independent of the distribution of bulk parameters and includes only ordinary differential equations, which could be easily solved numerically, as it was done, for example, in Shikhmurzaev (1993*a*) for the case

of gas/liquid/solid systems. However, here we will derive an approximate analytical expression describing the dependence of θ_d on parameters of the problem. Our analysis is based on the fact that for most liquids the parameter $\lambda \equiv \gamma\rho_0^s/\sigma$ is much greater than unity (see Shikhmurzaev 1993*a* for an order-of-magnitude analysis). Physically, it means that liquids cannot be considerably compressed even by intermolecular forces and do not tolerate considerable rarefaction so that the averaged density of a thin layer which contributes to the surface tension (the surface density) only slightly differs from the density of a corresponding layer in the bulk (this fact is also briefly mentioned in a well-known review by Dussan V. 1979).

So we may consider $\delta = {\lambda_1}^{-1}$ as a small parameter and use perturbation methods as $\delta \to 0$ with $k_\lambda \equiv \lambda_2/\lambda_1$ fixed. The same approach was applied in Shikhmurzaev (1994, 1996) to derive analytical expressions for θ_d in the case of gas/liquid/solid systems.

Expanding the functions in power series in δ as $\delta \to 0$ and substituting these expansions in (3.31) and (3.15), (3.16) (for $j = s$, $\theta = \theta_1$, θ_2), we obtain that, as expected, the leading terms of asymptotic expansions in δ which satisfy (3.25) are the same as in the case of a gas/liquid/solid system (Shikhmurzaev 1994) namely

$$\rho_i^s = \rho_{is}^s + \delta B_i \exp(-q_i r), \tag{4.6}$$

$$v_i^s = (-1)^{i-1} + \frac{\delta q_i {k_\tau}^{i-1} B_i}{4{V_i}^2} \exp(-q_i r) \quad \text{on } \theta = \theta_i; \quad i = 1, 2; \tag{4.7}$$

where

$$\begin{aligned} q_i &= 2{k_\tau}^{1-i} \frac{V_i}{(\rho_{is}^s)^{1/2}} \left(\left(\frac{{V_i}^2}{\rho_{is}^s} + 1 \right)^{1/2} + (-1)^i \frac{V_i}{(\rho_{is}^s)^{1/2}} \right) \\ &\approx 2{k_\tau}^{1-i} V_i \left(({V_i}^2 + 1)^{1/2} + (-1)^i V_i \right), \qquad i = 1, 2. \end{aligned}$$

Here B_1 and B_2 are the constants of integration, which can be determined by substituting (4.7) into (3.20):

$$\left.\begin{aligned} B_1 &= -\lambda_1(\rho_{1s}^s + \rho_{1f}^s u_{r(0)}(\theta_d, k_\mu)) \left(\frac{q_1}{4{V_1}^2} + 1 \right)^{-1}, \\ B_2 &= \lambda_1(\rho_{2s}^s - \rho_{2f}^s u_{r(0)}(\theta_d, k_\mu) - \rho_{res}^s) \left(\frac{q_2 k_\tau}{4{V_2}^2} - 1 \right)^{-1}. \end{aligned}\right\} \tag{4.8}$$

Then, substituting (4.7) into (3.21) and using (4.8) and (3.27), we can finally obtain an equation describing the dependence of the dynamic contact angle on the contact-line speed and other parameters:

$$\cos\theta_s - \cos\theta_d = \frac{2\lambda_1(\rho_{1s}^s + \rho_{1f}^s u_{r(0)}(\theta_d, k_\mu))}{(1 + 1/{V_1}^2)^{1/2} + 1} + \frac{2\lambda_2(\rho_{2s}^s - \rho_{2f}^s u_{r(0)}(\theta_d, k_\mu) - \rho_{res}^s)}{(1 + 1/{V_2}^2)^{1/2} - 1}. \tag{4.9}$$

Equation (4.9) includes the corresponding equations derived for gas/liquid/solid systems (Shikhmurzaev 1994, 1996) as well as some empirical relationships known in the literature as particular cases (see Hayes & Ralston 1993 for a review).

Equation (4.9) involves the following eleven non-negative parameters:

$$\theta_s, \lambda_1, \lambda_2, \rho_{1s}^s, \rho_{2s}^s, \rho_{1f}^s, \rho_{2f}^s, \rho_{res}^s, V_1, V_2, k_\mu, \tag{4.10}$$

which satisfy one constraint – (3.26). Besides this, ρ_{2s}^s and ρ_{res}^s appear in (4.9) as a combination $\rho_{2s}^s - \rho_{res}^s$, which therefore may be formally regarded as one parameter. Using (3.27), we may replace one of the first five parameters of (4.10) by p_S^s.

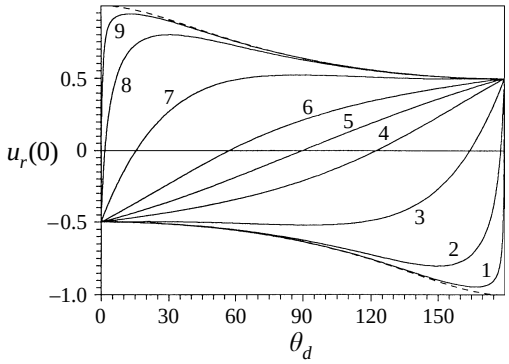

FIGURE 2. The free-surface velocity versus the dynamic contact angle for different viscosity ratios. Curves 1–9 correspond to $k_\mu = 10^{-3}$, 10^{-2}, 10^{-1}, 0.5, 1, 2, 10, 10^2, 10^3, respectively. Dashed lines are obtained for $k_\mu = 0, \infty$.

It should be emphasized that the present model in its general formulation does not imply any particular relationship between the dynamic contact angle and the contact-line speed. Equation (4.9) holds under the conditions listed above and also under an implicit assumption that the inner limit of the outer solution is given by (3.8). If (3.8) is not valid (for example, when the flow near the contact line is influenced by other closely located boundaries), the theory will lead to the so-called hydrodynamic assist of wetting – the effect observed experimentally by Blake, Clarke & Ruschak (1994).

5. Analysis

In this section we will briefly analyze some properties of (4.9).

The two terms on the right-hand side of (4.9) describe the contributions of the parameters of the two fluids resulting in the deviation of θ_d away from its static value θ_s. We will begin the analysis starting from the simplest case where the receding fluid is a viscous gas to reveal the role of the viscosity ratio only. The corresponding equation for the velocity dependence of θ_d may be formally obtained, for example, by setting $\lambda_2 = 0$ in (4.9). Comparing the result with the formula derived in Shikhmurzaev (1994) for the case of an ideal gas (the latter case for the problem considered here physically corresponds to a vacuum/liquid/solid system), we see that, as should be expected, the viscosity ratio k_μ appears only in the expression for the velocity of the free surface $u_{r(0)}(\theta_d, k_\mu)$ represented by the classical solution (3.8).

In the case of a viscous gas/liquid/solid system, the dynamic contact angle depends only on the following five parameters

$$\theta_s,\ V_1,\ \rho^s_{1f},\ p^s_{1S},\ k_\mu, \tag{5.1}$$

where for convenience ρ^s_{1s} is replaced by p^s_{1S} using (3.27) and (2.13) with $p^s_{2S} = 0$, while λ_1 becomes equal to $1/(1 - \rho^s_{1f})$ from (3.26). The role of the first four parameters in (5.1) is analysed in Shikhmurzaev (1993*a*).

Figure 2 shows $u_{r(0)}$ as a function of θ_d for different viscosity ratios (this figure is identical with figure 6 in Cox (1986) since the inner limit of the outer solution is the same for different models). As the dynamic contact angle grows and one moves along a curve in the $(\theta_d, u_{r(0)})$-coordinate plane starting from a point corresponding to some prescribed values of k_μ and θ_s, the flow character changes from the rolling motion of

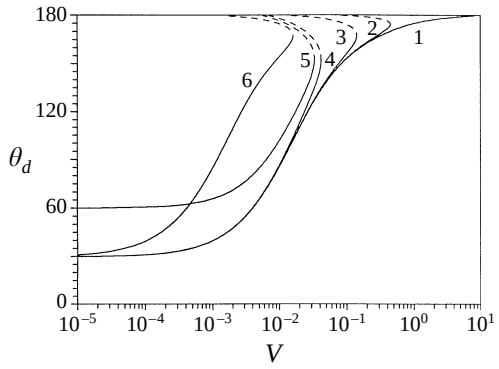

FIGURE 3. The velocity dependence of the macroscopic contact angle formed by an interface between a viscous gas and a liquid with a solid surface for different viscosity ratios. Curves 1–4 correspond to $k_\mu = 0,\ 10^{-4},\ 10^{-3},\ 10^{-2}$, respectively ($\theta_s = 30^\circ,\ \rho^s_{1f} = 0.99,\ p^s_S = 0$); 5, $\theta_s = 60^\circ,\ k_\mu = 10^{-2}$; 6, $\rho^s_{1f} = 0.999,\ k_\mu = 10^{-3}$. Dashed lines correspond to branches which have no physical meaning.

the advancing fluid ($u_{r(0)} < 0$) to that of the receding one. For low and high values of k_μ, the corresponding curve in the $(\theta_d, u_{r(0)})$-plane deviates from the dashed lines obtained for $k_\mu = 0, \infty$ only at the values of θ_d very close to 180° and 0°, respectively, i.e. when the domain occupied by the low-viscosity fluid is so thin that the viscosity of the fluid, however small, cannot be neglected.

Figure 3 presents the dynamic-contact-angle dependence on the contact-line speed in gas/liquid/solid systems for different values of k_μ. Curve 1 corresponds to a vacuum–liquid system, i.e. $k_\mu = 0$. The most important feature of the curves is that a solution of (4.9) exists only up to a certain finite value of $V_1 = V_{1max}$ (dashed lines in figure 3 show the branches which have no physical meaning). Strictly speaking, the presence of a maximum contact-line speed in the formulation, which assumes a steady motion of a straight contact line, means at least that either the contact line is no longer straight or that the motion is no longer steady. In this connection, it is reasonable to look at what happens in the experiments when a steady motion of a straight contact line breaks down. Experiments (Blake & Ruschak 1979) show that the breakdown of steady motion of a straight contact line corresponds to the onset of gas entrainment: the contact line takes a 'sawtooth' form, and small bubbles start to come off the angular points of the contact line and go into the bulk of the spreading liquid. Blake & Ruschak advanced the idea of a maximum speed of wetting V_*, according to which, if a liquid is forced to spread with a speed greater than V_*, the contact line takes a 'sawtooth' shape to make the normal component of the contact-line velocity equal to V_*. This concept of a 'maximum speed of wetting' excellently described the observed behaviour of the contact-line shape. It seems reasonable to associate V_{1max} with the maximum speed of wetting and the onset of gas entrainment. This may be called a 'severe' mechanism of the gas entrainment since one may also expect a 'soft' mechanism due to the hydrodynamic instability of the free surface.

As was shown in Shikhmurzaev (1993*a*, 1994), in a vacuum/liquid/solid system, a maximum speed of wetting may also exist but only either if $p^s_S > 0$ (in this case, it corresponds to $\theta_d = 180^\circ$) or if (2.5) is replaced by a more complicated equation of state. In a general situation, both factors will modify V_{1max}. It should be pointed out that the maximum contact-line speed was also obtained by Cox (1986), who considered the apparent contact angle (see the next section for details) assuming that

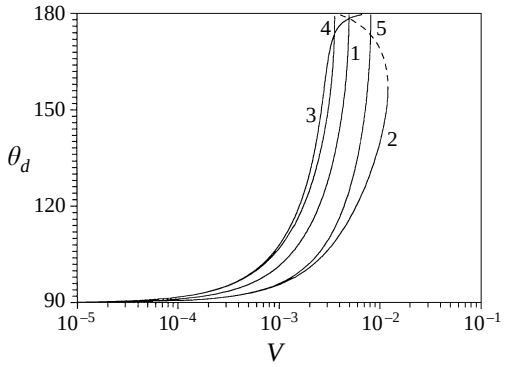

FIGURE 4. The velocity dependence of θ_d in liquid–liquid systems for different viscosity ratios, λ_1 and λ_2. $\rho^s_{1f} = \rho^s_{2f} = 0.99$. 1, $\lambda_1 = \lambda_2 = 50$, arbitrary k_μ; 2, $\lambda_1 = 90$, $\lambda_2 = 10$; 3, $\lambda_1 = 10$, $\lambda_2 = 90$; (2, 3, $k_\mu = 10^{-2}$); 4, $\lambda_1 = 90$, $\lambda_2 = 10$; 5, $\lambda_1 = 10$, $\lambda_2 = 90$; (4,5, $k_\mu = 10^2$); other parameters: $\theta_s = 90^\circ$, $k_V = 1$, $\rho^s_{1s} = \rho^s_{2s} = 1$, $p^s_S = 0$, $\rho^s_{res} = 0$.

$\theta_d \equiv \theta_s$. In his theory, the maximum contact-line speed corresponds to the apparent contact angle equal to 180°.

It should be mentioned that in experiments with gas/liquid/solid systems the viscosity ratio is usually very small (e.g. in a well-known work of Hoffman 1975, k_μ ranges from 10^{-5} to 10^{-8}) so that the curves obtained for $k_\mu = 0$ may be used to describe experimental data in a wide range of contact-line speeds. Nevertheless, even in this case, if the small-capillary-number approximation remains valid, the critical contact-line speed is determined by the viscosity ratio.

Now let us consider the behaviour of θ_d in liquid/liquid/solid systems. The parameters V_1 and V_2 may be interpreted as the contact-line speed made dimensionless by means of characteristic parameters of the advancing and receding liquid, respectively. We will use one of these parameters, say, V_1 as the dimensionless contact-line speed and a ratio

$$k_V = \frac{V_2}{V_1} \equiv \left[\frac{\beta_2 \rho^s_{10}(1 + 4\alpha_1\beta_1)}{\beta_1 \rho^s_{20}(1 + 4\alpha_2\beta_2)}\right]^{1/2}$$

instead of V_2.

As is clear from (4.9), only some parameters strongly effect the velocity dependence of θ_d. Indeed, λ_1 and λ_2 play the roles of the relative 'weights' of the two terms of the right-hand side of (4.9), and k_μ strongly affects the radial free-surface velocity $u_{r(0)}$, whilst the influence of the dimensionless equilibrium surface densities, which only slightly differ from unity, as well as of $\rho^s_{res} \ll 1$ should be relatively small.

In figure 4 the velocity dependence of θ_d for different k_μ, λ_1 and λ_2 is given. For a vivid illustration it is convenient to consider the case where $\rho^s_{1f} = \rho^s_{2f}$ (=0.99), $\theta_s = 90^\circ$, $p^s_S = 0$, so that (3.26), (3.27) give $\rho^s_{1s} = \rho^s_{2s} = 1$. The values of other parameters are given in the figure caption. Curve 1 corresponds to a symmetrical situation ($\lambda_1 = \lambda_2$) and an arbitrary value of k_μ. Thus, if the surface parameters of the two fluids are equal, the velocity dependence of θ_d is not affected by the viscosity ratio. The situation changes when $\lambda_1 \neq \lambda_2$. If $\lambda_1 \neq \lambda_2$ and $k_\mu \ll 1$, then even the qualitative behaviour of the curve $\theta_d = \theta_d(V_1)$ becomes dependent on the ratio $k_\lambda = \lambda_2/\lambda_1$ (see curves 2 and 3): for small k_μ and k_λ, like in the case of a gas/liquid/solid system, the curve $\theta_d = \theta_d(V_1)$ has a maximum contact-line speed corresponding to $\theta_d < 180^\circ$, while small k_μ and large k_λ give a completely different velocity dependence of θ_d.

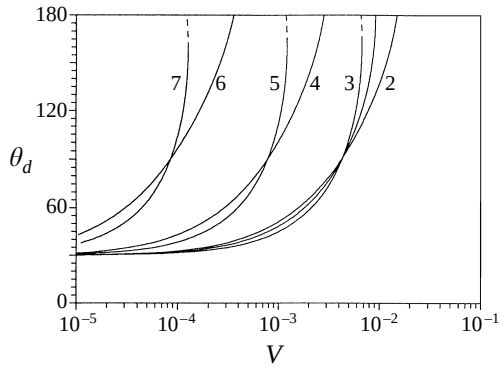

FIGURE 5. Dynamic contact angle versus contact-line speed for different λ_i and ρ^s_{if} ($i = 1, 2$). 1, $\lambda_1 = \lambda_2 = 50$; 2, $\lambda_1 = 10$, $\lambda_2 = 90$; 3, $\lambda_1 = 90$, $\lambda_2 = 10$ ($\rho^s_{1f} = \rho^s_{2f} = 0.99$ for curves 1–3); 4, $\lambda_1 = 50$, $\lambda_2 = 5 \times 10^2$; 5, $\lambda_1 = 5 \times 10^2$, $\lambda_2 = 50$; 6, $\lambda_1 = 50$, $\lambda_2 = 5 \times 10^3$; 7, $\lambda_1 = 5 \times 10^3$, $\lambda_2 = 50$ (for curves 1, 4–7 we have $\lambda_1(\rho^s_{1f} - 1) = \lambda_2(\rho^s_{2f} - 1)$). Other parameters: $\theta_s = 30°$, $k_V = 1$, $k_\mu = 1$, $\rho^s_{2s} = 1$, $p^s_S = 0$, $\rho^s_{res} = 0$.

If $k_\mu \gg 1$, then the curves in the (V_1, θ_d)-coordinate plane corresponding to small and large values of k_λ (curves 4, 5) behave in a similar manner (typical of the receding liquid flow in gas/liquid/solid systems with the contact angle measured through the gas (Shikhmurzaev 1996*a*)), though the values of the maximum contact-line speed at which $\theta_d = 180°$ may differ considerably. Comparing curves 1–5 in figure 4, we see that interchanging the roles of the fluids can lead to qualitative changes in the dynamic contact-angle behaviour if $\lambda_1 \neq \lambda_2$. Thus, the dynamic contact angle is strongly influenced not only by the viscosity ratio but also by the free-surface structure.

Figure 5 illustrates the role of the free-surface structure. For simplicity we use $k_\mu = 1$. It is interesting to know if the curves in the (V_1, θ_d)-coordinate plane depend on the relative contribution of the two fluids to the surface tension of the fluid–fluid interface (see (3.26)) or only on the values of λ_i ($i = 1, 2$). For $\lambda_1 = \lambda_2$ and $\rho^s_{1f} \neq \rho^s_{2f}$ (which implies different contributions of the fluids to the surface tension) the corresponding curves coincide with curve 1 within the graphical accuracy, as should be expected from (4.9). However, if $\lambda_1 \neq \lambda_2$ and the contributions of the fluids to the surface tension of the fluid–fluid interface are either equal (curves 1, 4–7) or different (curves 2, 3), then the velocity dependence of θ_d is strongly influenced by the direction of the fluid–liquid displacement. The intersection of different curves corresponds to the value of θ_d satisfying the equation $u_{r(0)}(\theta_d, k_\mu) = 0$.

Figure 6 presents the behaviour of $\theta_d(V_1)$ for different values of k_V and θ_s. For small k_V (curves 2, 5), a maximum displacement speed corresponds to $\theta_d < 180°$. This is not surprising since the case of a gas/liquid/solid contact line, where $\theta_d(V_{1max})$ is always less than 180° (see figure 3), can be formally obtained also by setting $k_V = 0$. For large k_V (curves 3, 6), the increase of $\theta_d(V_1)$ is not so rapid, and $\theta_d(V_{1max}) = 180°$.

The qualitative behaviour of the curves in the (V_1, θ_d)-coordinate plane is the same for different static-contact-angle values (curves 4–6), but the value of V_{1max} considerably decreases as θ_s grows.

Variations of p^s_S and ρ^s_{res} as well as of the equilibrium surface densities, which satisfy (3.26) and (3.27) for given λ_i ($i = 1, 2$) and θ_s, produce very small quantitative, and do not lead to any qualitative, changes of the curves in the (V_1, θ_d)-coordinate

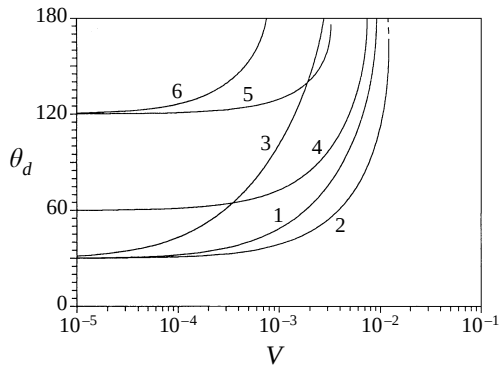

FIGURE 6. Dynamic contact angle versus contact-line speed for different k_V and θ_s. 1, 4, $k_V = 1$; 2, 5, $k_V = 0.1$; 3, 6, $k_V = 10$; 1–3, $\theta_s = 30°$; 4, $\theta_s = 60°$; 5, 6, $\theta_s = 120°$. Other parameters: $k_\mu = 1$, $\rho^s_{1f} = \rho^s_{2f} = 0.99$, $\lambda_1 = \lambda_2 = 50$, $\rho^s_{2s} = 1$, $\rho^s_{res} = 0$, $p^s_S = 0$.

plane. Recall that only the case of a 'thin' microscopic film is considered so that we may use values of ρ^s_{res} much less than unity.

Thus, the main features of the velocity dependence of the dynamic contact angle in fluid/liquid/solid systems are the following: the dynamic contact angle measured through the advancing fluid increases as the contact-line speed grows; for non-zero values of the viscosity ratio, there exists a finite maximum contact-line speed; the dynamic contact angle corresponding to the maximum contact-line speed may be equal to or less than 180°, and it is always less than 180° if the displaced fluid is a viscous gas.

Since in a number of experimental works the authors have reported the observed maximum contact-angle value equal to 180° for different fluid–liquid pairs and even for gas/liquid/solid systems, it is relevant to discuss the concept of 'contact angle' and the relations between the values of the contact angle defined in different ways in theoretical works and those measured in experiments.

6. Microscopic, macroscopic, apparent and effective contact angles

The term 'dynamic contact angle' is commonly used in the literature with different meanings, for example to describe processes of liquid–fluid displacement corresponding to essentially different characteristic dimensions of the flow domain, and here we will give more precise definitions of the concept and consider conditions of their applicability and peculiarities associated with the mathematical modelling of the liquid–fluid displacement on different length scales.

6.1. *Microscopic contact angle*

If the characteristic length scale (L) is comparable with the thickness of the interfacial layers (h), where the properties of contacting media strongly differ from those of the bulk due to the non-symmetrical action of intermolecular forces from the bulk phases experienced by molecules which form the interfacial layers, one may define a *microscopic* (or *actual*) contact angle θ_{act} (see figure 1*c*). This definition implies that the continuum mechanics approach remains applicable on such length scales, though the description of the three-phase interaction zone and the interfaces should take into account their diffuse nature: if $L \sim h$, then the usual 'interface', instead of being a geometrical surface with a surface tension, becomes the 'bulk' from the point

of view of continuum mechanics, and the forces of non-hydrodynamic origin should be explicitly taken into consideration. In this case, the main difficulty is to formulate the set of bulk hydrodynamic equations and, in particular, the equations describing the microscopic force field in the three-phase interaction zone. This problem in itself is extremely difficult so that the analysis of the liquid–fluid displacement in the framework of the new (microscopic) bulk equations becomes only an element of this general problem of microhydrodynamics. At present, only some aspects of wetting on the microscopic level are investigated (see de Gennes 1985 and Starov 1992 for reviews).

It should be pointed out that just the microscopic contact angle is usually obtained as a result of molecular dynamics simulation, where the macroscopic parameters are calculated using a length scale of averaging comparable with characteristic lengths associated with intermolecular interaction forces (Thompson & Robbins 1990).

6.2. *Macroscopic contact angle*

If $L \gg h$, then the usual hydrodynamic approach is applicable so that the interfaces may be modelled as geometrical surfaces of zero thickness possessing some intrinsic 'surface' properties, and the three-phase interaction zone becomes a structureless 'contact line' (figure 1*b*). In this case, the angle formed at the intersection of the tangent plane to the free surface at the contact line and the solid boundary may be called the *macroscopic* dynamic contact angle θ_d (figure 1*a*, *b*) since just θ_d is used as a geometric boundary condition for the macroscopic hydrodynamic equations determining the free-surface shape. The macroscopic contact angle is exactly the one considered by the Young equation, and just this angle is investigated in the present paper.

This angle is also studied in some works on wetting in the framework of the approach of chemical kinetics (Cherry & Holmes 1969; Blake & Haynes 1969; Blake 1993), which use the Young equation and relationship (4.5) for the driving force.

6.3. *Apparent contact angle*

If we are interested in an angle formed by the solid wall and the tangent plane to the free surface at a certain distance from the contact line, we come to the concept of an *apparent* contact angle θ_{app} (figure 1*a*). Although θ_{app} is not a characteristic of a model applied to describe the flow associated with moving contact lines, this angle is often used as an auxiliary concept in interpreting the results of experimental studies. The main idea is to consider bending of the free surface due to viscous stresses and relate the angle between the tangent plane to the free surface at a distance R from the contact line and the solid boundary with the macroscopic contact angle θ_d and the length scale s, on which details of how the shear-stress singularity is removed are essential (Dussan V. 1976), as

$$\epsilon \equiv \frac{s}{R} \to 0.$$

In the case of finite capillary numbers, θ_{app} becomes dependent on the overall flow while if $Ca \to 0$ and the flow in the vicinity of the contact line is not influenced by other closely located boundaries, one can obtain a universal relationship between θ_{app}, θ_d, Ca, and ϵ. This procedure for particular flows was considered by many authors (see, for example, Dussan V. 1976; Voinov 1976, 1978; Huh & Mason 1977*b*; Hocking 1977, 1981; Hocking & Rivers 1982) and in its most complete and general form has been reported by Cox (1986). Here we will briefly discuss how, if necessary, Cox's results could be connected with those obtained in the present paper.

Cox has shown that if

$$Ca\ln(\epsilon^{-1}) \to 0 \qquad \text{as } Ca \to 0, \epsilon \to 0, \tag{6.1}$$

then the asymptotic expansions in the 'outer' and 'slip' regions can be matched directly giving

$$\theta_{app} = \theta_d + O(Ca\ln(\epsilon^{-1})), \tag{6.2}$$

while if

$$Ca\ln(\epsilon^{-1}) = O(1) \qquad \text{as } Ca \to 0, \epsilon \to 0, \tag{6.3}$$

then an asymptotic region associated with coordinates $(\hat{r} = Ca\ln(\epsilon\tilde{r}), \theta)$ should be introduced between the 'outer' and 'slip' regions, and matching with three asymptotic regions gives

$$g(\theta_{app}, k_\mu) = g(\theta_d, k_\mu) + Ca\ln(\epsilon^{-1}) + O(Ca), \tag{6.4}$$

where

$$g(\theta, k) = \int_0^\theta \frac{\mathrm{d}\theta}{f(\theta, k)},$$

$$f(\theta, k) = \frac{2\sin\theta\{k^2(\theta^2 - \sin^2\theta) + 2k[\theta(\pi - \theta) + \sin^2\theta] + [(\pi - \theta)^2 - \sin^2\theta]\}}{k(\theta^2 - \sin^2\theta)[(\pi - \theta) + \sin\theta\cos\theta] + [(\pi - \theta)^2 - \sin^2\theta](\theta - \sin\theta\cos\theta)}$$

and the last terms on the right-hand sides of (6.2) and (6.4) depend on the particular geometry of the flow (e.g. spreading drop, meniscus in a tube, etc) and therefore show the relevance of considering the contact-line motion as a closed local problem. Here as before we are dealing with the leading terms of asymptotic expansions in ϵ and Ca as $\epsilon \to 0$, $Ca \to 0$.

Equation (6.4) (or (6.2) as the particular case) is a universal characteristic of the current state of the system since it does not require any specification of the model in the 'slip' region and involves only two parameters, which determine the shape of the flow domain in this region (θ_d) and the relative length corresponding to a non-classical boundary condition (ϵ). The accuracy of (6.4) has been verified numerically (Zhou & Sheng 1990).

However, if one is going to interpret (6.4) (or especially (6.2)) not as a characteristic of the current state with prescribed θ_d and ϵ but as the dependence of θ_{app} on the dimensionless contact-line speed (i.e. Ca), then some assumptions concerning the velocity dependence of θ_d and ϵ should be made or a specific model for the flow in the 'slip' region determining these parameters should be formulated.

In a number of works it is assumed that

$$\theta_d \equiv \theta_s, \quad \epsilon \equiv \text{const.} \tag{6.5}$$

These assumptions combined with (6.2) give that θ_{app} is always equal to θ_s independently of the contact-line speed, and this is in clear conflict with experimental observations, while substituting (6.5) into (6.4), one obtains θ_{app} as an increasing function of Ca. The latter case was thoroughly investigated by Cox (1986).

However, different authors (Zhou & Sheng 1990; Foister 1990; Stokes *et al.* 1990; Fermigier & Jenffer 1991), who compared (6.4), (6.5) with experimental data, have clearly shown that (6.5) are not suitable assumptions for the systems examined, and at least the velocity dependence of θ_d should be allowed. As has been emphasized by Zhou & Sheng (1990), who investigated numerically the dynamics of immiscible-fluid displacement in a capillary tube using two different specific models for the flow in

the 'slip' region, "any significant variation of θ_{app} observed at $Ca < 10^{-2.7}$ can be attributed to the variation of θ_d away from its static value". To obtain satisfactory agreement between (6.4) and experimental data, different authors involve different adjustable relationships instead of or in addition to (6.5), thus in fact using (6.4) only as a starting point for semiempirical correlations.

The general formulation given in §2 of the present paper makes it possible to solve a wetting problem as a whole so that the solution will allow one to obtain Cox's formulae for the apparent contact angle, when this quantity is of interest. So there is a natural way of combining Cox's results with those obtained in the previous sections of the present paper for the case of small ϵ and Ca. Indeed, the present theory describes in particular the flow in the 'slip' region, so we may use (4.9) with the corresponding expression for $u_{r(0)}$ and $\epsilon_1 = U\tau_1/R$ instead of (6.5). The dimensionless contact-line speed V_1 is related to Ca_1 by

$$V_1 = Ca_1 Yu, \quad Yu = \left[\frac{\sigma\tau_1\beta_1}{\lambda_1\mu_1^2(1+4\alpha_1\beta_1)}\right]^{1/2}, \tag{6.6}$$

and ϵ_1 can be rewritten as

$$\epsilon_1 = Ca_1 E, \quad E = \frac{\sigma\tau_1}{\mu_1 L}. \tag{6.7}$$

The parameters Yu and E depend only on characteristics of the advancing fluid and one easily measurable parameter of the liquid–liquid interface (σ). Certainly, (4.9), (6.6), (6.7) also include (6.5) as a particular case. Thus (4.9), (6.4), (6.6), (6.7) give a combination of the present theory with Cox's results and make it possible to calculate the apparent contact angle θ_{app} in the case when the macroscopic contact angle θ_d is velocity-dependent.

6.4. *Effective contact angle*

Thus far we have considered different definitions of the dynamic contact angle for the immiscible-fluid displacement on a perfectly smooth chemically homogeneous solid surface, and the definitions were associated with different ratios of the two lengths, h and L. If one considers a rough or/and chemically inhomogeneous solid surface, then even in the simplest case there appears at least one more length scale $\mathscr{L}$, which characterizes the size of the solid surface inhomogeneities. On the length scale large compared to $\mathscr{L}$ it becomes desirable to replace the (unsteady) flow over the actual rough or/and chemically inhomogeneous solid surface by the flow over some 'effective' smooth and homogeneous boundary with suitably reformulated boundary conditions on it. The contact angle which is involved in this formulation may be called the *effective* dynamic contact angle θ_{eff}. Particular cases of the solid surface inhomogeneities were considered in Hocking (1976), Huh & Mason (1977*a*), Jansons (1985, 1986, 1988), Joanny & Robbins (1990) on the basis of different models for the flow in the vicinity of the actual contact line.

The model developed in the present paper can also be used for the effective contact angle calculation (since we must come to the case of a perfectly smooth chemically homogeneous solid surface as $\mathscr{L} \to 0$ and face all the problems described in the previous subsections), though it looks as if for sufficiently rough surfaces and high flow rates the structure of inhomogeneities plays much more important role than the underlying model of the flow in the immediate vicinity of the actual contact line.

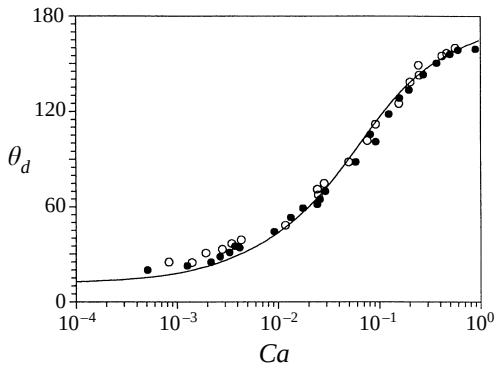

FIGURE 7. Comparison of the theory with experiments by Fermigier & Jenffer (1991) for a silicone–air interface in a capillary tube ($\theta_s = 12°$, $k_\mu = 3.6 \times 10^{-6}$: open circles, 47V5000 oil–air interface in a precision bore tube; filled circles, 47V5000 oil–air interface in a standard capillary tube; solid line, theoretical curve ($\log(Yu) = -0.58$).

7. Comparison with experimental data

In this section we will compare the theory with experimental data using (4.9), i.e. assuming that (6.1) is valid. In this case, (6.2) makes it possible to neglect the difference between θ_{app} and θ_d. This will allow us to understand if the velocity dependence of θ_d alone can be responsible for the variation of the experimentally measured contact angle away from its static value. Obviously, to use (6.4) instead of (6.2), we would only extend the set of theoretical curves and add one more (yet unknown and therefore adjustable) parameter.

All the parameters involved in the present theory have clear physical meanings and can be either directly or indirectly measured or calculated on the basis of a microscopic theory. For example, the relaxation times can be measured in other situations where interface formation or disappearance takes place (Bohr 1910; Kochurova *et al.* 1974). Using (2.3), we can also express the equilibrium surface densities in terms of the corresponding surface pressures, which are easily measurable quantities. A possible way of verifying or determining the surface equation of state is described in Shikhmurzaev (1996). However, at present the lack of information about some parameters does not allow us to carry out a comparison of the theory with experimental data using independently measured theoretical constants, and here we shall use some of them as adjustable parameters. Certainly, in this case, the comparison may be regarded as not more than preliminary, and we may speak only about the *possibility* of describing experimental data by (4.9). Below we will discuss how the number of adjustable parameters can be reduced.

In the case of gas/liquid/solid systems the situation is rather simple (Shikhmurzaev 1993*a*, 1994): since changes of ρ^s_{1f} lead to the same shifts of a theoretical curve in the semilogarithmic coordinates along the horizontal axis (figure 3) as the transition of coordinates from $(\log(V_1), \theta_d)$ to $(\log(Ca_1), \theta_d)$, we may fix the value of ρ^s_{1f} (say, equal to 0.99) and use $\log(Yu)$ as the only adjustable constant to describe the whole experimental curve (Yu stands for 'yet unknown'). The value of p^s_S becomes important only as θ_d approaches 180°, the value of λ_1 in this case is equal to $(1 - \rho^s_{1f})^{-1}$ (see (3.26)); ρ^s_{1s} can be calculated from (3.27). As shown in figure 7, the theory excellently fits to the experimental data obtained by Fermigier & Jenffer (1991) for a silicone oil–air interface in a capillary tube. Since both parameters ρ^s_{1f} and Yu are independent of the solid surface material, the same values of these parameters must be applicable

for the spreading of the same liquid over different solids (see Shikhmurzaev 1993*a*, where the theory is compared with the data for different gas/liquid/solid systems, for more details).

In the case of a liquid–liquid interface the situation is more complicated: we have four parameters, *Yu*, λ_1, λ_2 and k_V, each either producing a horizontal shift of a theoretical curve in the semilogarithmic coordinate plane or influencing, though very slightly, its slope (figures 4–6). At the same time all these parameters depend only on the liquid–liquid pair and should remain the same for different solid surfaces. So we will use two adjustable constants, *Yu* and k_λ, trying to fit simultaneously two theoretical curves to experimental data obtained for two different solid surfaces and the same liquid–liquid system. In order to eliminate the uncertainty in the remaining parameters it is reasonable to fix those which lead to the same horizontal shifts as *Yu* and propose some correlations between the others on the basis of some physical arguments consistent with the background of the present theory.

It is necessary to emphasize that the parameters involved in the present model are phenomenological by derivation, so that their values can be obtained either experimentally or from a more detailed structural theory. The correlations used below are not an essential part of the theory, and we invoke them simply to make the comparison of (4.9) with the data more restrictive.

So, let us fix, for example, ρ^s_{1f} and ρ^s_{2f} (say, $\rho^s_{1f} = \rho^s_{2f} = 0.99$) – then (3.26) will impose one constraint on λ_1 and λ_2, making possible only variations of k_λ.

An order-of-magnitude analysis of the coefficients involved in the theory, similar to that carried out in Shikhmurzaev (1993*b*) on the basis of a two-layer model of an interface, allows one to propose the following correlation between k_λ, k_V and k_μ:

$$k_V \propto \frac{k_\mu^{1/2}}{k_\lambda} G, \quad G = \frac{\gamma_2}{\gamma_1}\left[\frac{\rho_2(1+4\alpha_1\beta_1)}{\rho_1(1+4\alpha_2\beta_2)}\right]^{1/2}.$$

Here we have assumed that $\beta_i \propto \mu_i/h_i$, $\rho^s_{i0} \propto \rho_i h_i$ $(i = 1, 2)$, where h_i is the thickness of the interfacial sublayer in the ith liquid (figure 1*c*, *d*). The same estimates give $\alpha_i \propto h_i/\mu_i$, and inferring that the bulk parameters of the liquids are of the same order of magnitude, we will assume simply that

$$k_V = \frac{k_\mu^{1/2}}{k_\lambda} \tag{7.1}$$

and use this relationship to eliminate the uncertainty in the value of k_V. It should be pointed out that theoretical curves become insensitive to k_λ and k_V as the value of k_μ increases.

In figures 8 and 9 we have shown the results of comparing the theory with experimental data reported by Fermigier & Jenffer (1991) for a capillary flow of different glycerin–silicone oil systems in two different glass tubes. Since they examined liquid–liquid pairs which include the same advancing liquid and a series of homologous liquids of increasing viscosities as receding fluids we have claimed the requirement that k_λ behaves in a systematic way as the receding fluid viscosity grows as an additional constraint.

As is clear from figure 8 and 9, the theoretical curves described by (4.9) are in good agreement with the experimental data. It should be pointed out also that the present theory fits these experiments much better than (6.4), (6.5) even if the curves obtained from (6.4), (6.5) are shifted by a quantity corresponding to multiplying *Ca* by a suitably chosen factor (see Fermigier & Jenffer 1991 for details).

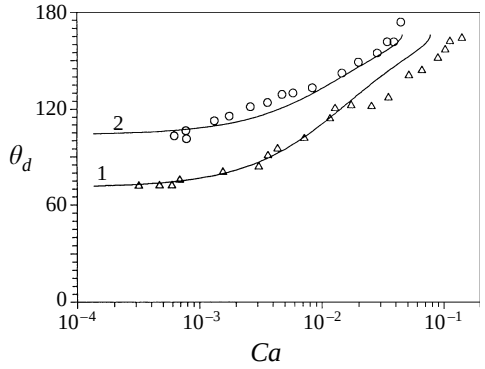

FIGURE 8. Comparison of the theory with experiments by Fermigier & Jenffer (1991) for a glycerin–47V2 oil interface in a capillary tube ($k_\mu = 1.35 \times 10^{-3}$): triangles, a precision bore tube ($\theta_s = 71°$); circles, a standard capillary tube ($\theta_s = 104°$); solid lines 1, 2, the present theory ($\log(Yu) = 0.1$, $k_\lambda = 1/9$ for both curves).

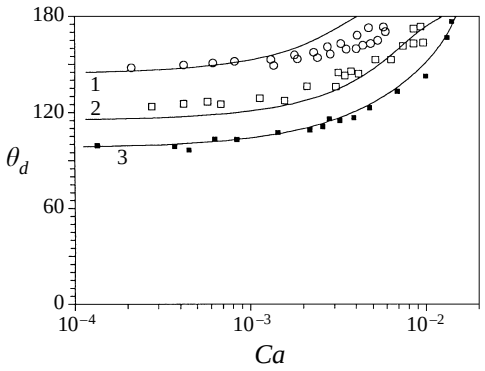

FIGURE 9. Comparison of the theory with experiments by Fermigier & Jenffer (1991) for different glycerin–silicone oil systems in a capillary tube: circles, glycerin–47V100 oil interface ($k_\mu = 1.0 \times 10^{-1}$) in a standard tube ($\theta_s = 144°$); open squares, glycerin–47V100 oil interface ($k_\mu = 1.0 \times 10^{-1}$) in a precision bore tube ($\theta_s = 115°$); filled squares, glycerin–47V1000 interface ($k_\mu = 9.0 \times 10^{-1}$) in a precision bore tube ($\theta_s = 98°$); solid lines, the present theory ($\log(Yu) = -0.55$, $k_\lambda = 4$ for curves 1 and 2; $\log(Yu) = -1.15$, $k_\lambda = 9$ for curve 3).

It is noteworthy also that a large static-contact-angle hysteresis observed in the cited experiments was attributed by the authors either "to a nonhomogeneous glass surface composition, or to the adsorption of a microscopic liquid film on the solid surface". While the former reason would lead to considerable discrepancy between the results obtained for a liquid–air interface in the same tubes and to the static-contact-angle hysteresis of the same order (but it is not so, see figure 7), the latter is in complete agreement with the present theory: though the presence of a 'thin' microscopic residual film can strongly affect the static contact angle (see (3.27)), its direct influence on the dynamic contact angle is very small (see (4.9) and §5).

In figure 10 we have shown the results of comparing the theory with experiments performed by Gutoff & Kendrick (1982) using a tape plunging into a pool of water with different immiscible oils as the upper (receding) fluid. A possible explanation of the discrepancy between curve 2 and the experimental data may be the rapid increase of ρ^s_{res} similar to that observed in the receding contact-line motion in gas/liquid/solid

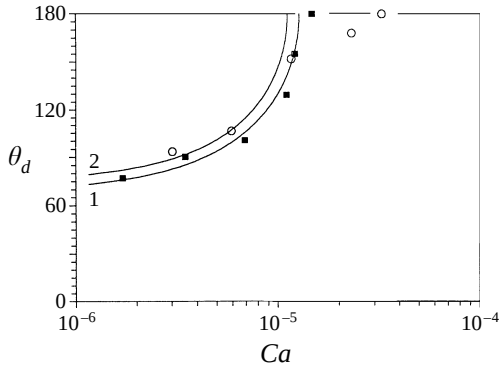

FIGURE 10. Comparison of the theory with experiments by Gutoff & Kendrick (1982) for a gelatine-subbed polyester tape moving across an interface between water and different oils: filled squares, water/castor oil ($\theta_s = 74°$, $k_\mu = 1021$); open circles, water/mineral oil ($\theta_s = 68°$, $k_\mu = 185$); solid lines, the present theory (1, $\log(Yu) = 1.8$; 2, $\log(Yu) = 2.1$; $k_\lambda = 1$ for both curves).

systems (see Shikhmurzaev 1996 for a discussion). Some ways of generalizing the theory to take this effect into account will be briefly described in §10.

It is necessary to point out that for small wetting rates (4.9) gives a linear dependence of $\cos\theta_s - \cos\theta_d$ on V_1. The same dependence results from the chemical-kinetics theory proposed by Blake & Haynes (1969) (see also its generalization in Blake 1993) and correlates with their experimental data. This is not surprising since both theories are based on closely related physical grounds.

Summing up the results presented in figures 7–10 we may conclude that the simplest theory formulated on the basis of the surface tension relaxation analysis is in reasonable agreement with experimental data.

8. Flow field

A general scheme of the flow near the moving contact line was considered in Huh & Scriven (1971) and Dussan V. & Davis (1974). Below we will investigate the fine structure of the flow in the 'intermediate' region in the framework of the present model for liquid–liquid displacement and focus our attention on the transition from the rolling motion of one liquid to that of another. An analysis of the flow in the liquid in the case of a gas/liquid/solid system can be found elsewhere (Shikhmurzaev 1996).

Substituting (4.7), (4.8) into (3.17) and using (3.28), (3.30) to simplify (3.18), one obtains the distributions of the radial components of velocities along the interfaces in the 'intermediate' region, and (3.19) gives the transversal ones:

$$\left.\begin{aligned} u_{ir}(r,\theta_i) = (-1)^{i-1} + \frac{\delta q_i B_i k_\tau^{i-1}}{2V_i^2(1+4A_i)}\exp(-q_i r) \qquad (i = 1.2), \\ u_{1r}(r,0) = u_{2r}(r,0) = u_{r(0)}(\theta_d, k_\mu) \qquad (i = 1,2), \\ u_{i\theta}(r,\theta) \equiv 0 \qquad \text{on } \theta = 0, \theta_i;\ i = 1,2, \end{aligned}\right\} \tag{8.1}$$

where θ_d is the solution of (4.9). The velocity distribution in the bulk can be computed from (3.10), (3.11), (8.1).

A convenient way of calculating the flow field is to rewrite (3.10), (3.11), (8.1) in terms of the stream functions and by using the Mellin transform reduce the

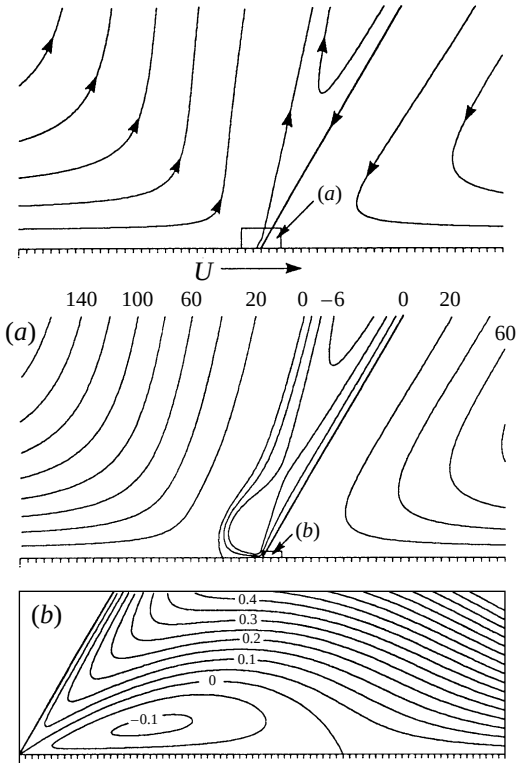

FIGURE 11. A typical example of the flow field shown as a series of magnified views. The numbers correspond to the stream function values. The curves are obtained for $\theta_s = 30^\circ$, $k_\mu = 1$, $\rho^s_{res} = 0$, $\rho^s_{1f} = \rho^s_{2f} = 0.99$, $k_V = 1$, $k_\lambda = 1$, $A_1 = A_2 = 0.1$, $k_\tau = 1$, $p^s_S = 0$.

problem to a standard boundary-value problem for two linear ordinary differential equations of the fourth order with constant coefficients, which can be easily solved analytically. Then the velocity field can be calculated after overcoming the usual difficulties inherent in the numerical inverse Mellin transform.

As is seen from (8.1) and illustrated in figures 11–13, generally there are two points on the liquid–solid interface where $u_r = 0$. Indeed, if

$$2\left(\rho^s_{is} + (-1)^{i-1}\rho^s_{if}u_{r(0)} + (1-i)\rho^s_{res}\right)\frac{(1+V_i^2)^{1/2} + (-1)^i V_i}{(1+V_i^2)^{1/2} - (-1)^i V_i} - (1+4A_i) > 0 \quad (i = 1,2), \tag{8.2}$$

then on the interface between the ith liquid and the solid, there is a stagnation point located at a distance

$$r_{0i} = \frac{1}{q_i}\ln(D_i), \quad D_i = (-1)^i \frac{\delta q_i k_\tau^{i-1} B_i}{2V_i^2(1+4A_i)} \qquad (i = 1,2) \tag{8.3}$$

from the origin. The fulfillment of (8.2) in the rolling liquid means that a vortex appears (figures 11, 13) due to the flow-induced Marangoni effect, i.e. the reverse influence of the surface tension gradient caused by the flow on the bulk velocity distribution. The same situation takes place in gas/liquid/solid systems at low

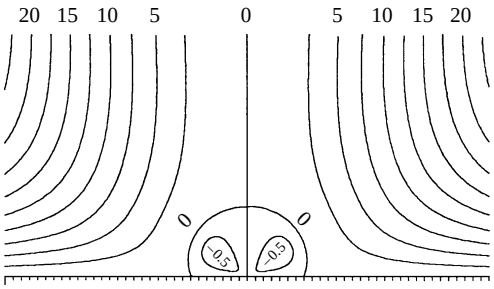

FIGURE 12. The transition of the flow regime. The radial velocity of the free surface is zero. The values of the parameters are the same as in figure 11.

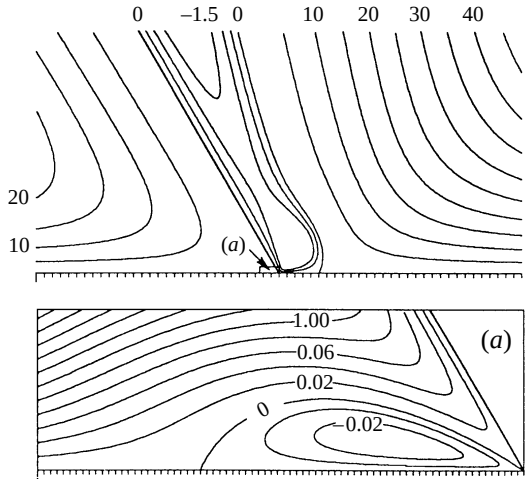

FIGURE 13. The receding liquid is rolling. The vortex in the advancing fluid has disappeared.

contact-line speeds and small contact angles for the advancing interface and at high speeds for the receding one (Shikhmurzaev 1996).

If (8.2) is met for the non-rolling liquid, then the separatrix of the flow field begins from a point located in the 'intermediate' region (figures 11, 13); otherwise it comes from the origin. We should remember that for the 'intermediate' region, the inner limit of the bulk velocity is not equal to zero and depends on the direction along which the point approaches the origin, and the term 'origin' means the 'inner' region. This multi-valuedness of the velocity at the origin in the 'intermediate' region (and hence the stress singularity) is eliminated in the 'inner' region, where the first terms on the left-hand sides of (2.2) and (2.9) cannot be neglected.

As the contact-line speed increases, θ_d approaches the value at which the transition of the flow regime takes place. We used $k_\mu = 1$ for the flow pattern given in figures 11–13 so that this value is equal to 90°. The transition corresponds to zero radial velocity of the points on the free surface and gives rise to a pair of co-rotating vortices near the origin (figure 12). The tendency to vortex formation in the receding fluid is clearly seen in figure 11. Then the region of closed streamlines in the advancing fluid 'opens' and its bounding streamline becomes the separatrix (figure 13). In figure 13 we can see the 'traces' of the former vortex.

9. The present model and existing theories

In this section we will try to address the following questions which may be of interest both to experts in the field and to potential users of the theory. What is the relationship of the present model, and in particular of the coefficient of sliding friction β, to other models which include slip? Is the introduction of 'extra' physical constants a serious drawback of the model? What are the advantages of the model compared to previous theories? And finally, is the model too complicated to be useful for engineering applications?

To answer these questions we have first to describe in brief existing hydrodynamic approaches to the wetting phenomenon, which allow one to consider it theoretically as a well-posed mathematical problem. A hydrodynamicist who faces the moving contact-line problem has to decide (A) how to describe the behaviour of the macroscopic contact angle (see §6 for the definition) and (S) how to remove the shear-stress singularity. In the literature devoted to the subject, one can find the following approaches to Problem A:

(A1) $\theta_d \equiv \theta_s$ (Dussan V. 1976; Hocking 1977, 1981, 1992; Huh & Mason 1977*b*; Davis 1980; Hocking & Rivers 1982; Cox 1986; Durbin 1988; Zhou & Sheng 1990)

(A2) $U = k(\theta_d - \theta_s)$, where k is an empirical constant (Greenspan 1978; Greenspan & McCay 1981; Davis 1980; Hocking 1990; Haley & Miksis 1991).

(A3) $U = k(\theta_d - \theta_s)^m$, where k and m are either purely empirical constants (Ehrhard & Davis 1991; Haley & Miksis 1991) or, developing the simple arguments of Tanner (1979), the results of an assumption concerning the asymptotic behaviour of the dynamic contact angle (Goodwin & Homsy 1991; Braun *et al.* 1995).

(A4) θ_d is prescribed, and its dependence on the contact-line speed and other parameters is not specified (Lowndes 1980; Levine *et al.* 1980; Tilton 1988; Finlow, Kota & Bose 1996).

(A5) $\theta_d \equiv 180^\circ$ (Benney & Timson 1980; Pismen & Nir 1982; Pukhnachev & Solonnikov 1982; Baiocchi & Pukhnachev 1990)

One can also find a generalization of (A2)–(A3), which takes into account the hysteresis of the static contact angle (Davis 1980; Hocking 1990).

The case (A5), artificial from the physical point of view though rather interesting mathematically, can be considered without relaxing the no-slip boundary condition [Benney & Timson 1980; Pukhnachev & Solonnikov 1982. See also Pismen & Nir (1982), which, taking account of a remark in Ngan & Dussan V. (1984) concerning the sign of the curvature, should be associated with the receding contact-line motion] implying that the other fluid is inviscid.

For $\theta_d \neq 180^\circ$ one has to replace the no-slip boundary condition near contact to get rid of the shear-stress singularity. The following approaches to the problem have been proposed:

(S1) $\boldsymbol{n} \cdot \boldsymbol{P} \cdot (\boldsymbol{I} - \boldsymbol{nn}) = \beta(\boldsymbol{u} - \boldsymbol{U})$ – the classical Navier boundary condition (Lamb 1932, p. 586), where for the coefficient of sliding friction one may use

(S1a) β = const (Hocking 1977, 1981, 1990, 1992; Huh & Mason 1977*b*; Davis 1980; Lowndes 1980; Levine *et al.* 1980; Hocking & Rivers 1982; Zhou & Sheng 1990; Ehrhard & Davis 1991; Haley & Miksis 1991).

(S1b) $\beta = \beta(h)$, where h is the distance between the free surface and the solid boundary (Greenspan 1978; Greenspan & McCay 1981; Goodwin & Homsy 1991; Haley & Miksis 1991; Braun *et al.* 1995).

(S1c) $\beta = 0$ if $r \leqslant U\tau$ and $\beta = \infty$ for $r > U\tau$ ('slip-stick' condition), where r is the distance from the contact line and τ is the relaxation time (Huh & Mason 1977*b*).

(S1d) $\beta = \infty$ if $|\boldsymbol{n}\cdot\boldsymbol{P}\cdot(\boldsymbol{I}-\boldsymbol{nn})| < T_*$ and $\beta = T_*/|\boldsymbol{u}-\boldsymbol{U}|$ otherwise ('yield-stress' condition), where T_* is the yield stress (Durbin 1988).

(S2) Prescribed the distribution of the fluid velocity along the solid surface (l is the slip length)

(S2a) $u = Ur/(l+r)$ (Dussan V. 1976),

(S2b) $u = Ur^2/(l^2+r^2)$ (Dussan V. 1976),

(S2c) $u = Ur^{1/2}/(l^{1/2}+r^{1/2})$ (Dussan V. 1976),

(S2d) $u = U(1-\exp(-r/l))$ (Zhou & Sheng 1990; Finlow *et al.* 1996).

(S3) $u = U$ for $r \geqslant l$ while for $r < l$ the distribution of the velocity of the fluid along the solid surface is the one which provides the minimum for the entropy production in the bulk (Baiocchi & Pukhnachev 1990).

To complete the picture of existing hydrodynamic theories we have to mention semiempirical approaches which either cut off the neighbourhood of the contact line together with the shear-stress singularity, which is attributed to the breakdown of continuum mechanics modelling, and prescribe the value of the contact angle at the cut-off distance from the contact line (Voinov 1976, 1978, 1995; Boender, Chesters & Zanden 1991) or, understanding the existing difficulty, replace the analysis of what happens in the vicinity of the contact line by introducing the apparent contact angle at a certain distance from the contact line as an empirical function of the contact-line speed and other parameters of the problem (Kafka & Dussan V. 1979; Ngan & Dussan V. 1989; Dussan V., Ramé & Garoff 1991). Although semiempirical approaches may be a good tool for a particular experiment, they of course provide no understanding of the phenomenon. It is also worth mentioning that according to recent experiments (Chen, Ramé & Garoff 1995), the free-surface slope at a certain distance from the contact line as a function of the contact-line speed is not sufficient to describe the free-surface shape since as the contact-line speed increases, the hydrodynamics of the flow in the vicinity of the contact line 'appears in the field of view' (as should be expected from the present theory, where the relaxation length $l = U\tau$ increases with the contact-line speed).

A schematic review of purely empirical correlations can be found in Hayes & Ralston (1993).

There is also a great number of works which assume the existence of a film ahead of the spreading liquid thus removing the singularity together with the contact line itself. For obvious reasons those works are not reviewed here.

As we see from the picture given above, the existing theories treat problems A and S separately and therefore require two independent assumptions about the dynamic contact angle and the way to remove the singularity so that in principle every combination of A's and S's will give a new theory! The situation is obviously unsatisfactory, and probably therefore some authors are employing different A–S models simultaneously trying to point out their common or specific features (Dussan V. 1976; Huh & Mason 1977*b*; Davis 1980; Zhou & Sheng 1990; Haley & Miksis 1991) or use purely empirical approaches (Kafka & Dussan V. 1979; Ngan & Dussan V. 1989; Dussan V. *et al.* 1991).

In contrast to the A–S models, the present theory is based on the consideration of a more general phenomenon – the interface formation process – and, being derived from first principles, provides a solution of the moving contact-line problem as a by-

product so that both sides of this problem, description of the dynamic-contact-angle behaviour and elimination of the shear-stress singularity, appear to be related.

An essential feature of the A–S models is that they have either to use the assumption (A1), which is in conflict with experimental observations (see §6 and references therein), or to include purely empirical constants (see (A2) and (A3)) or even functions (see (A4), which implies a prescribed velocity-dependence of θ_d on U and other parameters). Obviously, the presence of empirical constants or functions considerably reduces the predictive power of a model and excludes the possibility of determining parameters of the model from independent experiments not associated with wetting. In contrast, the present theory includes only physical constants with clear physical meanings (Shikhmurzaev 1993*a*, *b*). These constants can be measured with the help of different experimental methods involving interface formation or disappearance, not necessarily associated with wetting. One such method is that of an oscillating jet, which originates from Bohr's (1910) formula and allows one to determine the dynamic surface tension (Kochurova *et al.* 1974). Some possible ways of determining the parameters of the model are discussed also in Shikhmurzaev (1996).

It should be also emphasized that any particular relationship between the dynamic contact angle and the contact-line speed excludes the possibility of describing the hydrodynamic assistance of wetting (Blake *et al.* 1994) in principle, since, roughly speaking, this effect means that there is no such relationship (see also a remark at the end of §4).

A common feature of conditions (S1)–(S3), except (S2c), is that they describe the fluid motion near the contact line as sliding†, thus implying that the contact line always consists of the same material elements, while experiments show that it should be rolling (see (i) in §1). The present model starts from and obviously preserves the rolling character of the flow.

At the same time, although the present model was derived from the first principles (Shikhmurzaev 1993*a*, *b*) and may seem distant from the early theories, we must emphasize that the 'seeds' of this model are present in many of them. Indeed, (A2)–(A4) replace the Young equation and – since the Young equation, being simply the tangential momentum conservation law, remains of course valid – imply that the surface tensions of a contacting interface near the contact line are not in equilibrium when the contact line is moving. Consistently developing this idea, one would arrive at a model similar to that described in the present paper. Furthermore, the exponential velocity distribution postulated in (S2d) is a particular case of (8.1), where the length l involved in (S2d) is specified (however, in the 'inner' asymptotic region, where the first term on the left-hand side of (2.2) becomes important, the velocity distribution will be of course different).

Logical development of the S3 model would also lead to a theory similar to or even more general than the present one. Indeed, if in addition to the entropy production in the bulk one were to take into account the corresponding contribution from the interfaces (the latter component becomes more important as the contact line is approached especially in the case of small capillary numbers), then the variations of the surface energies, and hence the surface tensions, along the interfaces would be involved in the analysis resulting in the consideration of the interface formation process similar to that employed in the present paper.

† Sometimes, as in the case of (S1c), the actual flow field implied by a model is in conflict with the physical idea which motivated the model derivation (see Dussan V. 1979 for details).

The A1–S1a model requires special attention not only as the most popular but in the current context because mathematically this model is the limiting case of the present theory if $\tau_i = 0$ $(i = 1, 2)$. Indeed, if $\tau_i = 0$, then the surface tension relaxation occurs within the contact line and hence $\theta_d \equiv \theta_s$ while the second term on the right-hand side of (2.2) becomes zero and (2.2) coincides with (S1)-(S1a). Mathematically β in (S1a) is equivalent to β_i in (2.2). In both cases, this coefficient allows for slip in the vicinity of the contact line and thus removes the shear-stress singularity at the angular point of the flow domain. However, we have to emphasize two essential points.

First, the physical backgrounds for the coefficient of sliding friction in (S1a) and in the present theory are completely different. It is often supposed that "physical reasons lying behind a condition like (S1)–(S1a) are probably connected with roughness of the solid surface, either on a macroscopic or molecular level" (Hocking 1992). This argument is applicable to a particular case of macrohydrodynamic 'wetting' of very rough solid surfaces at high flow rates where the details of the actual contact-line motion are not important, and the apparent 'wetting' is due to the free surface bending so that the free surface successively passes over the surface roughness elements thus producing the impression of the 'effective' contact line motion (Hocking 1976). However, in a general case, roughness of the solid surface reduces slip even if perfect slip is assumed on the microscopic level (Richardson 1973; Jansons 1988). The idea of actual slip on the hydodynamic level is also in conflict with the results of the molecular dynamics simulations (Koplik, Banavar & Willemsen 1988, 1989; Thompson & Robbins 1989).

On the contrary, the present model, in agreement with the results of molecular dynamics simulations, does not require any actual slip, and β characterizes the properties of an interfacial layer (the layer which contributes to the surface tension) and allows for apparent slip on the liquid-facing side of the interface. As is clear from the order-of-magnitude analysis given in Shikhmurzaev (1993*a*), under usual conditions the shear stress is unable to produce measurable slip of a viscous liquid on a solid surface while the surface tension gradient can do this. It should be pointed out also that in general the second term on the left-hand side of (2.2) is more important and just this term is responsible for the deviation of the dynamic contact angle away from the static value and, in the case of small Ca, for the force between the liquid and the solid in the vicinity of the contact line (see (4.1), (4.5)).

The second point concerning (2.2) and (S1) is the bulk pressure singularity at the contact line which becomes integrable when a slip boundary condition is applied but still is not removed. Of course this singularity, due to its integrability, is not an obstacle for practical applications of the models, but its origin should be understood. The pressure singularity as well as the stagnation point at the edge of the flow domain is inherent in every mathematical model which introduces the contact line as a singularity in the curvature of the flow domain boundary. Of course, in nature, every boundary, including an artificial surface separating the 'interface' and the 'bulk' is smooth as far as the continuum mechanics length scale is considered (see curve Q in figure 4 in Shikhmurzaev 1994), and the boundary conditions along them vary gradually, thus excluding any singularity. Introduction of a flow domain confined by a simple piecewise smooth boundary with piecewise smooth boundary conditions is a considerable simplification, which becomes possible at best at the expense of the bulk pressure singularity if the shear-stress density has a non-zero limit as the contact line is approached. This can be shown using the results of Kondrat'ev (1967) and Maz'ya & Plamenevskii (1973).

In this connection, an essential strong point of the present theory, in contrast to (S1), is that in principle it allows one to smooth the angular point of the flow domain boundary and drop the first term on the left-hand side of (2.2) everywhere without changing its macroscopic characteristics (Shikhmurzaev 1991*b*; see also p. 55 in Shikhmurzaev 1994). Thus, introduction of the shear stress in (2.2) at small Ca may be regarded simply as a 'payment' for the simplification of the shape of the flow domain, though at large Ca, when θ_d approaches 180°, this term can play an important role.

Now let us consider the practical aspects of using the present theory. In the case of gas/liquid/solid systems, which is most important for applications, the model is very simple. There are only two non-dimensional parameters specific to the model, namely the non-dimensional contact-line speed V_1, which is related to Ca_1 by (6.6), and the surface density ρ^s_{1f} characterizing the equilibrium state of the free surface, plus the tangential component of the force acting on the contact line p^s_{1S}, which will be common for all models employing the Young equation instead of empirical correlations like (A2) or (A3). Those physical parameters can be determined from independent experiments. Alternatively, one can use experiments on wetting and determine those parameters from one experimental curve for a given liquid and then apply the values obtained to describe a family of curves corresponding to the spreading of this liquid over different solids (see figure 13 in Shikhmurzaev 1993*a*). One can also use an algebraical equation relating θ_d to the contact-line speed and other parameters both for the advancing and receding contact-line motion (Shikhmurzaev 1994, 1996). Application of the present model to a particular problem is illustrated in Shikhmurzaev (1997).

The case of a liquid/liquid/solid system is much more complex since one has to take into account the specific interaction of each liquid with the solid surface as well as their interaction with each other, and of course it would be naive to expect that such a complicated system with very rich behaviour can be described by a few constants. In this case, the present theory characterizes the system by eight independent non-dimensional constants specific to the model (see (4.10), (3.26)), though, as is shown in §5, the flow is strongly influenced only by a few of them. One can also use the simple algebraical equation (4.9), which relates θ_d to those parameters, and equation (4.5) for the force between the liquids and the solid near the contact line. It should be emphasized that the fact that the model contains only physical (but not empirical) constants gives an important advantage since, as was pointed out above, these constants can be determined with the help of experiments not necessarily associated with wetting and used to describe other flows of the same liquids where the classical approach leads to physically unacceptable singularities.

Finally, it should be noted, especially in connection with liquid–liquid displacement, where sometimes even experimental results are rather contradictory (see, for example, Dussan V. 1977; Brown, Jones & Neustadter 1980; Savelski *et al.* 1995), that oversimplification of a mathematical model at the expense of its ability to describe this very complex phenomenon seems hardly desirable.

10. Concluding remarks

10.1. *Limitations of the theory*

Natural limitations of the present theory are those inherent in the hydrodynamic approach itself. According to the definition of this approach (see §1), the intermolecular

forces are hidden in the transport coefficients, relaxation times, etc, which appear as averaged macroscopic quantities, and microhydrodynamic length scales associated with those forces are neglected. These simplifications give important advantages for considering particular macroscopic problems but at the same time impose limitations on the applicability of hydrodynamic theories. If the characteristic dimensions of the flow domain L or the 'slip length' $U\tau$ become comparable with the interfacial layer thickness h (which is nelected in hydrodynamics where the interfaces are treated as geometrical surfaces of zero thickness), the present model becomes inapplicable and a suitable generalization of it which provides a more detailed (structural) description of interfaces must be used. This is also necessary when the dynamic contact angle measured either through the advancing or receding liquid approaches zero since in this limit every microhydrodynamic length, say, h introduces a macroscopic length scale h/θ_d so that the three-phase interaction zone is no longer a one-dimensional 'contact line' from a hydrodynamic point of view. This argument is well-known in the mechanics of thin films, where flows of the films may be considered in the framework of conventional hydrodynamics, while the process of their rupture and the formation of a hole or a dry spot is investigated taking into account long-range intermolecular forces.

10.2. *Generalization of the model*

As is clear from its derivation (Shikhmurzaev 1993*a*, *b*), the above-described model is the simplest one that can be derived using true kinematics of the flow and the idea of relaxation of the surface tension as a physical basis. As is shown in the previous sections, the model eliminates the shear-stress singularity and is in reasonable agreement with experimental data.

Different possible ways of how the model may be generalized were briefly described in Shikhmurzaev (1993*a*, 1994) for the case of liquid–gas displacement, and below we will discuss some questions which are specific for liquid/liquid/solid systems.

First is the role of a microscopic residual film. In the present paper we assumed that the film is 'thin' so that it was sufficient to take it into account only in the mass balance condition for the surface phase (see (2.11) and (3.20)) and characterize it only by two constants ρ^s_{res} and p^s_{res}. However, in the case of a 'thick' microscopic residual film, it will influence not only the mass balance at the contact line but also the properties of the interface between the advancing fluid and the solid. A 'thick' microscopic residual film may be responsible for peculiarities of the velocity-dependence of the dynamic contact angle observed in some experiments. A possible way of taking this film into account is to introduce a two-layer model of the liquid–solid interface similar to that applied for the free-surface description.

The second problem is associated with the influence of the structure of the three-phase interaction zone on the flow. In the present paper we assumed that (i) there are only surface mass fluxes along interfaces, thus neglecting possible mass exchange between the three-phase interaction zone and the bulk, and (ii) there is no resistance to 'splitting' of the liquid–liquid interface at the moving contact line and to the mass transfer across the three-phase interaction zone. The two constraints imply a very simple structure of the contact-line region. A study of the three-phase interaction region would give more general conditions at the contact line. At the same time, at present there are no indications concerning physical mechanisms which should be additionally incorporated in the model.

Finally, we must make special remarks about the concept of the surface density and the surface tension relaxation process. In the present model ρ^s is not used as a measure

of inertia of an interface: it is considered simply as a quantity which characterizes the state of the interface. Both the surface density and the surface tension are determined by the non-symmetric action of intermolecular forces on the molecules of an interface. We use (2.3) as the simplest possible surface equation of state. Certainly, we could eliminate ρ^s using (2.3) and deal directly with the surface tension relaxation equation, which may be proposed as a starting point of the theory. We could also interpret ρ^s as the surface density of a surfactant if it is present in excess in the bulk and determines the surface tension. One may propose more complicated surface equation of state and include the influence of other parameters which characterize the interface state, for example the ordering of molecules in the interfacial layer. At the same time, on the basis of the analysis given in the previous sections we may conclude that at present the simplest theory is able to describe experimentally observed features of wetting phenomena, and we have to get additional information from experiments which would allow us to generalize the model.

More important is the question about the value of τ, which characterizes the interface formation time. In the present theory we assumed that τ_i are large enough that the deviation of θ_d from the static contact angle takes place, and the surface tension relaxation length becomes macroscopic. This assumption is supported not only by experiments on wetting, which show that, indeed, $\theta_d \neq \theta_s$, but also by independent measurements of the surface tension relaxation time (see Posner & Alexander 1949; Kochurova *et al.* 1974 and references therein), which show that, both for solutions and pure liquids, the interface formation time is macroscopic. In this connection, experimental studies of the whole spectrum of flows, where interface formation or disappearance take place, are desirable, and they could provide addtional information about the characteristic time scale of the interface formation process.

REFERENCES

Baiocchi, C. & Pukhnachev, V. V. 1990 Problems with one-side limitations for Navier–Stokes equations and the dynamic contact-angle problem *J. Appl. Mech. Techn. Phys.* (Russia) No. 2, 27–40.

Bedeaux, D., Albano, A. M. & Mazur, P. 1976 Boundary conditions and non-equilibrium thermodynamics. *Physica* A **82**, 438–462.

Benney, D. J. & Timson, W. J. 1980 The rolling motion of a viscous fluid on and off a rigid surface. *Stud. Appl. Maths* **63**, 93–98.

Blake, T. D. 1993 Dynamic contact angles and wetting kinetics. In *Wettability* (ed. J. C. Berg), pp. 251–309. Marcel Dekker, Inc.

Blake, T. D., Clarke, A. & Ruschak, K. J. 1994 Hydrodynamic assist of dynamic wetting. *AIChE J.* **40**, 229–242.

Blake, T. D. & Haynes, J. M. 1969 Kinetics of liquid/liquid displacement. *J. Colloid Interface Sci.* **30**, 421–423.

Blake, T. D. & Ruschak, K. J. 1979 A maximum speed of wetting. *Nature* **282**, 489–491.

Boender, W., Chesters, A. K. & Zanden, A. J. J. van der 1991 An approximate analytical solution of the hydrodynamic problem associated with an advancing liquid-gas contact line. *Intl J. Multiphase Flow* **17**, 661–676.

Bohr, N. 1910 Determination of the tension of a recently formed water-surface. *Proc. R. Soc. Lond.* A **84**, 395–403.

Braun, R. J., Murray, B. T., Boettinger, W. J. & McFadden, G. B. 1995 Lubrication theory for reactive spreading of a thin drop. *Phys. Fluids* **7**, 1797–1810.

Brown, C. E., Jones, T. D. & Neustadter, E. L. 1980 Interfacial flow during immiscible displacement. *J. Colloid Interface Sci.* **76**, 582–586.

Chen, Q., Ramé, E. & Garoff, S. 1995 The breakdown of asymptotic hydrodynamic models of liquid spreading at increasing capillary number. *Phys. Fluids* **7**, 2631–2639.

CHERRY, B. W. & HOLMES, C. M. 1969 Kinetics of wetting of surfaces by polymers. *J. Colloid Interface Sci.* **29**, 174–176.

COX, R. G. 1986 The dynamics of the spreading of liquids on a solid surface. Part 1. Viscous flow. *J. Fluid Mech.* **168**, 169–194.

DAVIS, S. H. 1980 Moving contact lines and rivulet instabilities. Part 1. The static rivulet. *J. Fluid Mech.* **98**, 225–242.

DURBIN, P. A. 1988 Consideration on the moving contact line singularity with application to frictional drag on a slender drop. *J. Fluid Mech.* **197**, 157–169.

DUSSAN V., E. B. 1976 The moving contact line: the slip boundary condition. *J. Fluid Mech.* **77**, 665–684.

DUSSAN V., E. B. 1977 Immiscible liquid displacement in a capillary tube. The moving contact line. *AIChE J.* **23**, 131–133.

DUSSAN V., E. B. 1979 On the spreading of liquids on solid surfaces: static and dynamic contact lines. *Ann. Rev. Fluid Mech.* **11**, 371–400.

DUSSAN V., E. B. & DAVIS, S. H. 1974 On the motion of a fluid-fluid interface along a solid surface. *J. Fluid Mech.* **65**, 71–95.

DUSSAN V., RAMÉ, E. & GAROFF, S. 1991 On identifying the appropriate boundary conditions at a moving contact line: an experimental investigation. *J. Fluid Mech.* **230**, 97–116.

EHRHARD, P. & DAVIS, S. H. 1991 Non-isothermal spreading of liquid drops on horizontal plates. *J. Fluid Mech.* **229**, 365–388.

ELLIOTT, G. E. P. & RIDDIFORD A. C. 1967 Dynamic contact angles. I. The effect of impressed motion. *J. Colloid Interface Sci.* **23**, 389–398.

FERMIGIER, M. & JENFFER, P. 1991 An experimental investigation of the dynamic contact angle in liquid-liquid systems. *J. Colloid Interface Sci.* **146**, 226–241.

FINLOW, D. E., KOTA, P. R. & BOSE, A. 1996 Investigations of wetting hydrodynamics using numerical simulations. *Phys. Fluids* **8**, 302–309.

FOISTER, R. T. 1990 The kinetics of displacement wetting in liquid/liquid/solid systems. *J. Colloid Interface Sci.* **136**, 266–282.

GENNES, P. G. DE 1985 Wetting: statics and dynamics. *Rev. Mod. Phys.* **57**, 827–863.

GOODWIN, R. & HOMSY, G. M. 1991 Viscous flow down a slope in the vicinity of contact line. *Phys. Fluids* A **3**, 515–528.

GREENSPAN, H. P. 1978 On the motion of a small viscous droplet that wets a surface. *J. Fluid Mech.* **84**, 125–143.

GREENSPAN, H. P. & MCCAY, B. M. 1981 On the wetting of a surface by a very viscous fluid. *Stud. Appl. Maths* **64**, 95–112.

GUTOFF, E. B. & KENDRICK, C. E. 1982 Dynamic contact angles. *AIChE J.* **28**, 459–466.

HALEY, P. J. & MIKSIS, M. J. 1991 The effect of the contact line on droplet spreading. *J. Fluid Mech.* **223**, 57–81.

HANSEN, R. J. & TOONG, T. Y. 1971 Interface behavior as one fluid completely displaces another from a small-diameter tube. *J. Colloid Interface Sci.* **36**, 410–413.

HAYES, R. A. & RALSTON, J. 1993 Forced liquid movement on low energy surfaces. *J. Colloid Interface Sci.* **159**, 429–438.

HOCKING, L. M. 1976 A moving fluid interface on a rough surface. *J. Fluid Mech.* **76**, 801–817.

HOCKING, L. M. 1977 A moving fluid interface. Part 2. The removal of the force singularity by a slip flow. *J. Fluid Mech.* **79**, 209–229.

HOCKING, L. M. 1981 Sliding and spreading of two-dimensional drops. *Q. J. Mech. Appl. Maths* **34**, 37–55.

HOCKING, L. M. 1990 Spreading and instability of a viscous fluid sheet. *J. Fluid Mech.* **211**, 373–392.

HOCKING, L. M. 1992 Rival contact-angle models and the spreading of drops. *J. Fluid Mech.* **239**, 671–681.

HOCKING, L. M. 1995 The wetting of a plane surface by a fluid. *Phys. Fluids* **7**, 1214–1220.

HOCKING, L. M. & RIVERS, A. D. 1982 The spreading of a drop by capillary action. *J. Fluid Mech.* **121**, 425–442.

HOFFMAN R. 1975 A study of the advancing interface. I. Interface shape in liquid-gas systems. *J. Colloid Interface Sci.* **50**, 228–241.

Huh, C. & Mason, S. G. 1977*a* Effect of surface roughness on wetting (theoretical). *J. Colloid Interface Sci.* **60**, 11–38.

Huh, C. & Mason, S. G. 1977*b* The steady movement of a liquid meniscus in a capillary tube. *J. Fluid Mech.* **81**, 401–419.

Huh, C. & Scriven, L. E. 1971 Hydrodynamic model of steady movement of a solid/ liquid/fluid contact line. *J. Colloid Interface Sci.* **35**, 85–101.

Jansons, K. M. 1985 Moving contact lines on a two-dimensional rough surface. *J. Fluid Mech.* **154**, 1–28.

Jansons, K. M. 1986 Moving contact lines at non-zero capillary numbers. *J. Fluid Mech.* **167**, 393–407.

Jansons, K. M. 1988 Determination of the macroscopic (partial) slip boundary condition for a viscous flow over a randomly rough surface with a perfect slip boundary condition microscopically. *Phys. Fluids* **31**, 15–17.

Joanny, J. F. & Robbins, M. O. 1990 Motion of a contact line on a heterogeneous surface. *J. Chem. Phys.* **92**, 3206–3212.

Kafka, F. Y. & Dussan V., E. B. 1979 On the interpretation of the dynamic contact angle in capillaries. *J. Fluid Mech.* **95**, 539–565.

Kochurova, N. N., Shvechenkov, Yu. A. & Rusanov, A. I. 1974 Determination of the surface tension of water by the oscillation jet method. *Colloid J.* (*USSR*) **36**, 785–788.

Kondrat'ev, V. A. 1967 Asymptotics of solution of the Navier-Stokes equation near the angular point of the boundary. *Prikl. Matem. Mekh.* (*J. Appl. Maths Mech.*) **31**, No. 1, 119–123.

Koplik, J., Banavar, J. R. & Willemsen, J. F. 1988 Molecular dynamics of Poiseuille flow and moving contact lines. *Phys. Rev. Lett.* **60**, 1282–1285.

Koplik, J., Banavar, J. R. & Willemsen, J. F. 1989 Molecular dynamics of a fluid flow at solid surfaces. *Phys. Fluids* A **1**, 781–794.

Lamb, H. 1932 *Hydrodynamics.* Dover.

Levine, S., Lowndes, J., Watson, E. J. & Neale, G. 1980 A theory of capillary rise of a liquid in a vertical cylindrical tube and in a parallel-plate channel. Washburn equation modified to account for the meniscus with slippage at the contact line. *J. Colloid Interface Sci.* **73**, 136–151.

Lowndes, J. 1980 The numerical simulation of the steady movement of a fluid meniscus in a capillary tube. *J. Fluid Mech.* **101**, 631–645.

Marmur, A. 1983 Equilibrium and spreading of liquids on solid surfaces. *Adv. Colloid Interface Sci.* **19**, 75–102.

Maz'ya, V. G. & Plamenevskii, B. A. 1973 On asymptotics of solutions of the Navier-Stokes equations near wedges. *DAN SSSR, Ser. Mat. Fiz.* **210**, No. 1, 803–806.

Ngan, C. G. & Dussan V., E. B. 1984 The moving contact line with a 180° degree advancing contact angle. *Phys. Fluids* **27**, 2785–2787.

Ngan, C. G. & Dussan V., E. B. 1989 On the dynamics of liquid spreading on solid surfaces. *J. Fluid Mech.* **209**, 191–226.

Pismen, L. M. & Nir, A. 1982 Motion of a contact line. *Phys. Fluids* **25**, 3–7.

Posner, A. M. & Alexander, A. E. 1949 A new technique for determination of dynamic surface tensions. *Trans. Farad. Soc.* **45**, 651–661.

Pukhnachev, V. V. & Solonnikov, V. A. 1982 On the problem of dynamic contact angle. *Prikl. Matem. Mekh.* (*J. Appl. Maths Mech.*) **46**, 961–971.

Richardson, S. 1973 On the no-slip boundary condition. *J. Fluid Mech.* **59**, 707–719.

Savelski, M. J., Shetty, S. A., Kolb, W. B. & Cerro, R. L. 1995 Flow patterns associated with steady movement of a solid/liquid/fluid contact line. *J. Colloid Interface Sci.* **176**, 117–127.

Shikhmurzaev, Y. D. 1991*a* Hydrodynamics of wetting. The displacement of a gas by a liquid from a solid surface (invited lecture). In *Mater. 7th All-Union Congress on Theor. & Appl. Mechanics, Moscow, 15-21 Aug. 1991*, p. 368 [in Russian].

Shikhmurzaev, Y. D. 1991*b* Spreading flow of a viscous liquid over a solid surface. *Sov. Phys. Dokl.* **36**, 749–752.

Shikhmurzaev, Y. D. 1993*a* The moving contact line on a smooth solid surface. *Intl J. Multiphase Flow* **19**, 589–610.

Shikhmurzaev, Y. D. 1993*b* A two-layer model of an interface between immiscible fluids. *Physica* A **192**, 47–62.

SHIKHMURZAEV, Y. D. 1994 Mathematical modeling of wetting hydrodynamics. *Fluid Dyn. Res.* **13**, 45–64.

SHIKHMURZAEV, Y. D. 1996 Dynamic contact angles in gas/liquid/solid systems and flow in vicinity of moving contact line. *AIChE J.* **42**, 601–612.

SHIKHMURZAEV, Y. D. 1997 Spreading of drops on solid surfaces in a quasi-static regime. *Phys. Fluids* (accepted).

STAROV, V. M. 1992 Equilibrium and hysteresis contact angles. *Adv. Colloid Interface Sci.* **39**, 147–173.

STOKES, J. P., HIGGINS, M. J., KUSHNICK, A. P., BHATTACHARYA, S. & ROBBINS, M. O. 1990 Harmonic generation as a probe of dissipation at a moving contact line. *Phys. Rev. Lett.* **65**, 1885–1888.

TANNER, L. 1979 The spreading of silicone oil drops on horizontal surfaces. *J. Phys.* D **12**, 1473–1484.

TELETZKE, G. F., DAVIS, H. T. & SCRIVEN, L. E. 1988 Wetting hydrodynamics. *Revue Phys. Appl.* **23**, 989–1007.

THOMPSON, P. A. & ROBBINS, M. O. 1989 Simulation of contact-line motion: slip and the dynamic contact angle. *Phys. Rev. Lett.* **63**, 766–769.

THOMPSON, P. A. & ROBBINS, M. O. 1990 To slip or not to slip? *Phys. World* **3**, No. 11, 35–38.

TILTON, J. N. 1988 The steady motion of an interface between two viscous liquids in a capillary tube. *Chem. Engng Sci.* **43**, 1371–1384.

VOINOV, O. V. 1976 Hydrodynamics of wetting. *Fluid Dyn.* **11**, 714–721.

VOINOV, O. V. 1978 Asymptote to the free surface of a viscous liquid creeping on a surface and the velocity dependence of the angle of contact. *Sov. Phys. Dokl.* **23**, 891–893.

VOINOV, O. V. 1995 Motion of line of contact of three phases on a solid: Thermodynamics and asymptotic theory. *Intl J. Multiphase Flow* **21**, 801–816.

ZHOU, M. Y. & SHENG, P. 1990 Dynamics of immiscible fluid displacement in a capillary tube. *Phys. Rev. Lett.* **64**, 882–885.